Journal of Statistical Theory and Applications (2025) 24:275–305
https://doi.org/10.1007/s44199-025-00110-5

RESEARCH ARTICLE

# An Enhanced EWMA Model for Statistical Insights in Process Monitoring with Application in Brake Pad Failure and Carbon Fiber Strength

**Muhammad Waqas[1,7] · Song Hua Xu[2,3] · Syed Masroor Anwar[4] · Zahid Rasheed[5] · Gilbert Masengo[6]**

Received: 11 March 2024 / Accepted: 25 February 2025 / Published online: 16 April 2025


## Abstract

Conventional control charts often assume normality, which may not hold for many engineering processes. In cases where processes follow an Inverse Maxwell (IM) distribution, as seen in various industrial applications, it becomes crucial to employ suitable monitoring methods. To address this gap, this study introduces the hybrid exponentially weighted moving average ($HEWMA_{IM}$) chart for the IM distribution. Performance evaluation includes metrics like average run length, median run length, and standard deviation run length. Comparative analysis with existing IM distribution-based charts such as the Shewhart V chart ($V_{IM}$), exponentially weighted moving average ($EWMA_{IM}$), and extended EWMA ($EEWMA_{IM}$) charts reveal the $HEWMA_{IM}$ chart's superior efficiency. Real-world applications in brake pad production and carbon fiber strength testing validate its practicality and engineering applications. In conclusion, $HEWMA_{IM}$ is a novel tool tailored to monitor IM processes efficiently, offering enhanced process monitoring for diverse industries.

Extended author information available on the last page of the article

## Graphical abstract

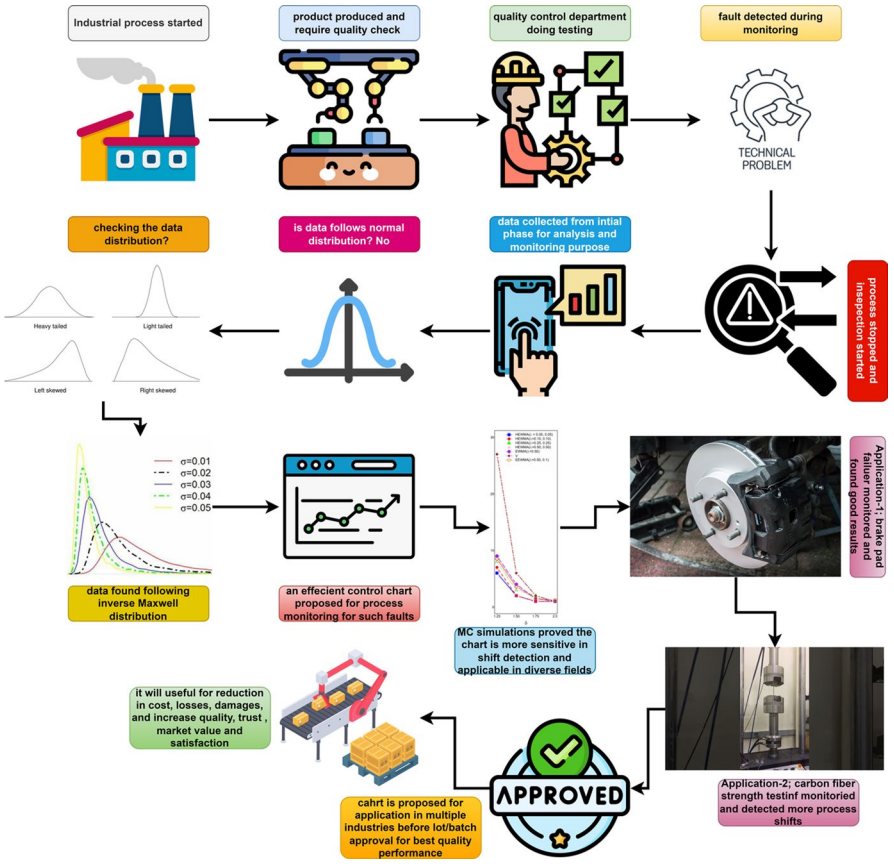


**Keywords** Control chart · Robustness · Process monitoring · Performance evaluation · Average run length · Engineering applications

## Abbreviations

| | |
|---|---|
| SPC | Statistical process control |
| EWMA | Exponentially weighted moving average |
| CUSUM | Cumulative sum |
| IM | Inverse Maxwell |
| EEWMA | Extended EWMA |
| HEWMA | Hybrid EWMA |
| RL | Run length |
| ARL | Average run length |
| RARL | Relative ARL |
| EQL | Extra quadratic loss |
| PCI | Performance comparison index |

OOC Out-of-control
IC In-control

## 1 Introduction

Control charts are beneficial for improving manufacturing quality; they can be used to eliminate waste and rework, which affect any business. This results in both an increase in productivity and a cost reduction. These charts are effective at preventing errors and maintaining process control. The idea behind it is always to do things correctly the first time. Classifying both good and bad products costs more than producing only good products. Control charts also limit the need for process modifications and tell the difference between general or specific variation causes. Variations are natural in all manufacturing processes, but these variations can occasionally exhibit high irregularity, resulting in an out-of-control (OOC) process. Statistical process control (SPC) is a toolkit that includes approaches for monitoring, managing, and improving a manufacturing process.

SPC is commonly used to monitor various processes by employing charts to detect OOC situations as soon as possible. Many control charts are introduced by quality experts, such as Shewhart-type charts, first given by Shewhart [62], which are utilized to detect large shifts. In contrast, cumulative sum (CUSUM) charts presented by Page [47] and exponentially weighted moving average (EWMA) charts by Roberts [55], respectively, are used to detect small and moderate shifts. Shewhart charts use only current information in their structure, so they are named memoryless charts. CUSUM and EWMA charts use current and previous information in their designs, which are termed as memory-type charts. In recent years, researchers modified the basic structure of memory-type charts to boost their performance further. One of them is the hybrid charts, which efficiently monitor the shifts in the process parameters (location and scale). In this regard, Haq [19] introduced the concept of hybrid exponentially weighted moving average (HEWMA) charts by combining the two EWMA charts so that one EWMA statistic is input to the other EWMA statistic. Later, Aslam et al. [12] demonstrated the usefulness of the HEWMA chart over conventional EWMA charts by employing the Conway-Maxwell Poisson distribution for count data. Likewise, Haq [20] constructed the HEWMA chart more efficiently than the classical CUSUM, EWMA, and mixed EWMA-CUSUM (MEC) charts for small shift detection. Furthermore, Aslam et al. [11] suggested the HEWMA chart for efficient monitoring of process dispersion. Also, Noor et al. [44] described a Bayesian HEWMA chart under various symmetric and asymmetric loss functions for improved process monitoring. Recently, X. Liu et al. [35–37] and Rasheed et al. [52] presented HEWMA structure-based charts for efficient process monitoring.

Usually, memory-type charts are used when the process data follow the normal distribution [33]. Sometimes, we may face a situation when the process data does not follow the normal distribution assumption [5]. Many researchers proposed charts for monitoring such skewed processes. For example, Hossain et al. [22] presented the Shewhart structure based $V_{IM}$ chart for process monitoring. Later,

Arafat et al. [8] designed the IM EWMA (IMEWMA) chart, which is more efficient than the $V_{IM}$ chart for small to moderate shift detection. Furthermore, Hossain et al. [24] constructed the VCUSUM chart based on Maxwell distribution features, outperforming the Shewhart V chart. Also, Omar et al. [45] advocated a Shewhart control chart for the IM process. Likewise, De la Torre-Gutiérrez and Pham [18] introduced a pattern reorganization system for feedback control in a skewed process environment, Yadpirun Supharakonsakun [71] provided the solution to the autoregressive processes, Saghir et al. [56] presented a new EWMA chart for process variance, and Hussain et al. [25] reinforced phase-I monitoring of location parameter for data containing outliers. Phase-I establishes a baseline and ensures the process is stable by identifying and eliminating special causes of variation. Phase-II is used for ongoing monitoring to detect deviations from the established control limits, ensuring the process remains stable. Zaka et al. [73] shaped the control chart for power function distribution, Shafqat et al. [59] designed a neutrosophic double and triple EWMA chart, and Ashraf et al. [10] gave the idea of a DEWMA memory chart for disease risk monitoring rather than using the memoryless disease detection methods. Additionally, Abbasi [1] improved the detection ability of the CV chart by using auxiliary information, Rasheed et al. [53] developed mixed memory charts for the process mean, and Zwetsloot et al. [74] monitored multivariate time between events. Also, Alevizakos et al. [3] presented triple EWMA signed-rank chart to measure process location, Phanthuna et al. [49] assessed a both-sided modified EWMA chart by using exact run length, Malela-Majika et al. [39] focused on robust non-parametric HEWMA chart for simple random and ranked set sampling to deal with normal and skewed data, and Boaventura et al. [15] proposed AI-based robust chart for better pattern detection by ignoring its sample scenario which is capable of large scale monitoring of industrial processes.

In a recent investigation, Rasheed et al. [51] gave the idea of a double EWMA chart for process location monitoring by combining the non-parametric and rank set sampling techniques, which performed better than its competing charts. Later, Xuechen Liu et al. [35–37] provided hybrid EWMA charts to process dispersion monitoring for normally distributed data and compared their efficiency with existing HEWMA charts. Moreover, Arslan et al. [9] gave a chart that estimates the unknown location shift using HEWMA statistic to deal with bias in mean shift and then adaptively update the smoothing parameter. Furthermore, work by M. Khan et al. [29, 31] utilizing the HWMA and double HWMA chart gave the idea of a triple HWMA chart for process dispersion monitoring. Additionally, Noor-ul-Amin et al. [43] presented a max-EWMA chart for joint monitoring of mean and variance,Sarwar et al. [57] anticipated the idea of Weibull monitoring of AEWMA chart,Rasheed et al. [52] provided EAEWMA chart for engineering sector monitoring and Jalilibal et al. [27] proposed charts for monitoring of high dimensional data streams. The literature on the double EWMA (DEWMA) chart has been examined by numerous researchers, including [32, 38, 42, 61]. Through an extensive literature review, we noted that various studies have utilized the DEWMA structure in different scenarios; however, no research has been conducted on situations following the inverse Maxwell distribution.

Recently, the HEWMA chart has gained popularity for its superior efficiency compared to the classical EWMA chart, particularly in process monitoring [29–31, 35–37, 73]. Similarly, the scope of applications for IM distribution is expanding that finding common use in health, agriculture, statistical mechanics, industrial processes, and various other fields [34, 48, 63, 65]. Furthermore, the contributions of Riaz et al. [54], Arafat et al. [8], Maqsood et al. [40] for IM process monitoring have established a significant base in the field, which also supports the extension for an enhanced memory charts to better support relevant industries. Therefore, the lack of an $HEWMA_{IM}$ chart for monitoring the IM process reveals an important research gap. Taking motivation from the work of Haq [19] and Ali and Haq [4], this study seeks to address this gap by introducing a $HEWMA_{IM}$ chart. This proposed chart fills an important gap in the existing literature, offering a valuable tool for effectively monitoring IM processes. By doing so, it aims to fulfill the specific requirements of industries that depend on these phenomena. To evaluate the performance of the proposed $HEWMA_{IM}$ chart against other control charts, specific performance evaluation measures such as average run length (ARL), median run length (MDRL) and standard deviation run length (SDRL) are used. For overall performance analysis, extra quadratic loss (EQL), performance comparison index (PCI), and relative ARL (RARL) measures are considered. Besides, an algorithm is designed in R using the Monte Carlo simulations method to calculate the performance evaluation measures. Existing control charts, such as $EWMA_{IM}$, $V_{IM}$, and $EEWMA_{IM}$ charts are considered for comparison. Moreover, the proposed control chart is implemented with two real-life applications to show practical importance.

The remainder of the manuscript is structured as follows: the design structures of the existing and proposed $HEWMA_{IM}$ charts are presented in Sect. 2. Section 3 discusses how the proposed chart implementation is performed. A comparative study is given in Sect. 4. Section 5 discusses the effectiveness of the proposed chart in detail using two real-life studies, while Sect. 6 shows the study's concluding remarks and some recommendations.

## 2 Design Structures of Existing and Proposed Control Chart

This section describes the design structures of existing and proposed charts under IM distribution. SubSect. 2.1 presents the design methodology of the Shewhart chart ($V_{IM}$) whereas SubSects. 2.2 and 2.3 explain the design structures of the other existing $EWMA_{IM}$ and $EEWMA_{IM}$ charts and SubSect. 2.4 presents the proposed $HEWMA_{IM}$ charts based on IM distribution, respectively.

### 2.1 $V_{IM}$ Chart

Omar et al. [45] investigated the features of the IM distribution and introduced the $V_{IM}$ chart, which is based on the Shewhart structure. Assume that X is a random variable with the Maxwell distribution, and the probability density and cumulative distribution function are as follows,

$$f(x,\boldsymbol{\sigma}) = \sqrt{\frac{2}{\pi}}\boldsymbol{\sigma}^{-3}x^2e^{\frac{-x^2}{2\sigma^2}};\ x>0 \tag{1}$$

$$F(x) = \frac{2}{\sqrt{\pi}}\gamma\left(\frac{3}{2},\frac{x^2}{2\boldsymbol{\sigma}^2}\right) \tag{2}$$

where $\int_0^u x^{v-1}e^{-\mu x}dx = \mu^{-v}\gamma(v,\mu u)$. By using the inverse transformation of the random variable X, the probability density function for the IM distribution is transformed as,

$$f(r,\boldsymbol{\sigma}) = \sqrt{\frac{2}{\pi}}\boldsymbol{\sigma}^{-3}r^{-4}e^{-\frac{1}{2r^2\sigma^2}};\ r>0 \tag{3}$$

where $X = \sqrt{\frac{2}{\theta}}\boldsymbol{\sigma}R$ and the cumulative distribution function is defined as,

$$F(r) = \frac{2}{\sqrt{\pi}}\left[1-\gamma\left(\frac{3}{2},\frac{1}{2r^2\boldsymbol{\sigma}^2}\right)\right];\ r>0 \tag{4}$$

Hence, the plotting statistic of a $V_{IM}$ chart is as,

$$V_{IM} = (3n)^{-1}\sum_{i=1}^{n}\frac{1}{r_i^2} = \frac{3nV_{IM}}{2\boldsymbol{\sigma}^2} = \sum_{i=1}^{n}P_i \tag{5}$$

The mean and variance of (5) are $E[V_{IM}] = \boldsymbol{\sigma}^2$ and $Var(V_{IM}) = \frac{2\boldsymbol{\sigma}^4}{3n}$, respectively. The control limits for the $V_{IM}$ chart is as,

$$\left.\begin{aligned} LCL &= E[V_{IM}] - L\times SD(V_{IM}) = \left[1-L\sqrt{\tfrac{2}{3n}}\right]\boldsymbol{\sigma}^2 = W_1\boldsymbol{\sigma}^2\\ CL &= E[V_{IM}] = \boldsymbol{\sigma}^2\\ UCL &= E[V_{IM}] + L\times SD(V_{IM}) = \left[1+L\sqrt{\tfrac{2}{3n}}\right]\boldsymbol{\sigma}^2 = W_2\boldsymbol{\sigma}^2 \end{aligned}\right\} \tag{6}$$

where $W_1 = \left[1-L\sqrt{\frac{2}{3n}}\right]$, $W_2 = \left[1+L\sqrt{\frac{2}{3n}}\right]$ and L denotes the false alarm rate. The process goes OOC if $V_{IM} < LCL$ or $V_{IM} > UCL$, otherwise, it will remain in an in-control (IC) state. The process is supposed to be statistically in an IC state if it is working under random cause variations, whereas a control chart illustrates a predefined average run length that characterizes the IC process (ARL0). If the process is in an IC state, then $\delta = 0$, otherwise, if the process is OOC state, $\delta \neq 0$.

### 2.2 $EWMA_{IM}$ Chart

Arafat et al. [8] presented the $EWMA_{IM}$ chart to monitor the scale parameter of IM distribution using $V_{IM}$ statistic. The plotting statistic of the $EWMA_{IM}$ chart is given as,

$$E_i = \lambda_1 V_{IM_i} + (1-\lambda_1)E_{i-1} \tag{7}$$

where $\lambda_1 \in (0,1]$ is a smoothing constant and $E_{i-1}$ are the previous observations. The mean and variance of the statistic $E_i$ are $E(E_i) = \sigma^2$ and $\mathrm{Var}(E_i) = \frac{2\sigma^4}{3n}\left\{\frac{\lambda_1}{2-\lambda_1}\left(1-(1-\lambda_1)^{2i}\right)\right\}$, respectively. The control limits based on this mean and variance are given below, when $\sigma^2$ is known

$$\left.\begin{array}{c} LCL_{(EWMA_{IM})i} = W_1\sigma^2 \\ CL_{(EWMA_{IM})i} = \sigma^2 \\ UCL_{(EWMA_{IM})i} = W_2\sigma^2 \end{array}\right\} \tag{8}$$

when $\sigma^2$ is unknown, we estimate $V_{IM}$ with the use of the following limits,

$$\left.\begin{array}{c} LCL_{(EWMA_{IM})i} = W_1\overline{V}_{IM} \\ CL_{(EWMA_{IM})i} = \overline{V}_{IM} \\ UCL_{(EWMA_{IM})i} = W_2\overline{V}_{IM} \end{array}\right\} \tag{9}$$

where $W_1 = 1 - L\sqrt{\frac{2}{3n}\left(\frac{\lambda_1}{2-\lambda_1}\left(1-(1-\lambda)^{2i}\right)\right)}$, $W_2 = 1 + L\sqrt{\frac{2}{3n}\left(\frac{\lambda_1}{2-\lambda_1}\left(1-\left(1-\lambda_1\right)^{2i}\right)\right)}$, where L is the control chart constant. The process remains IC if $LCL_{(EWMA_{IM})i} < E_i < UCL_{(EWMA_{IM})i}$, else it is OOC.

### 2.3 $EEWMA_{IM}$ Chart

Maqsood et al. [40] gave the EEWMA chart for non-normal distributions, specifically targeting positively skewed IM distribution. The statistical measure used for plotting in the EEWMA control chart, a customized extension, is defined as follows. The current observation is assigned a positive weight, while the preceding observations are assigned a negative weight, which reflects its distinct adaption from the traditional EWMA, defined as,

$$u_i = \alpha_1 V_{1M_i} - \alpha_2 V_{1M_{i-1}} + (1-\alpha_1+\alpha_2)u_{i-1} \tag{10}$$

The values of the smoothing constant $\alpha_1$ and $\alpha_2$ ranges between $0 < \alpha_1 \le 1$, $0 < \alpha_2 \le 1$, respectively.

The $\mu$ and $\sigma^2$ of $EEWMA_{IM}$ chart is given as,

$$\begin{aligned} E(u_i) &= \sigma^2 \\ \mathrm{Var}(u_i) &= \frac{2\sigma^4}{3n}\left(\alpha_1^2+\alpha_2^2\right)\left[\left\{\frac{1-a^{2i}}{2(\alpha_1-\alpha_2)-(\alpha_1-\alpha_2)^2}\right\} - \left\{\frac{1-a^{2i-2}}{2(\alpha_1-\alpha_2)-(\alpha_1-\alpha_2)^2}\right\}\right] \end{aligned} \tag{11}$$

So, the control structure LCL, CL and UCL for $EEWMA_{IM}$ chart derived by using $\mu$ and $\sigma^2$ mentioned above.

### 2.4 Proposed $\mathbf{HEWMA_{IM}}$ Chart

Following Haq [19] and Ali and Haq [4], we introduced the $\mathrm{HEWMA_{IM}}$ chart for monitoring scale parameters of IM distribution. Let $\{\mathrm{HE_i}\}$ for $\mathrm{i} \geq 1$ be the sequence of observations based on the other sequence $\{\mathrm{E_i}\}$, then, the plotting statistic $\mathrm{HE_i}$, for the $\mathrm{HEWMA_{IM}}$ chart is defined as

$$\left.\begin{aligned} \mathrm{E_i} &= (1-\lambda_1)\mathrm{E_{i-1}} + \lambda_1 \mathrm{V_{IM_i}}, \quad 0 < \lambda_1 \leq 1 \\ \mathrm{HE_i} &= (1-\lambda_2)\mathrm{HE_{i-1}} + \lambda_2 \mathrm{E_i}, \; 0 < \lambda_2 \leq 1 \end{aligned}\right\} \tag{12}$$

where $\lambda_1$ and $\lambda_2$ are smoothing constants. The initial values of $\mathrm{HE_i}$ and $\mathrm{E_i}$ are set to $\sigma^2$ that is, $\mathrm{HE_0} = \mathrm{E_0} = \sigma^2$. The mean and variance of $\mathrm{HE_i}$ are respectively, given as

$$\left.\begin{aligned} &\mathrm{E}(\mathrm{HE_i}) = \sigma^2 \\ &\mathrm{V}(\mathrm{HE_i}) = \left(\frac{\lambda_1\lambda_2}{\lambda_1-\lambda_2}\right)^2 \left[ \begin{array}{c} \sum_{\mathrm{i}=1}^{2} \frac{(1-\lambda_i)^2\left\{1-(1-\lambda_i)^{2\mathrm{t}}\right\}}{1-(1-\lambda_i)^2} - \\ \frac{2(1-\lambda_1)(1-\lambda_2)\left\{1-(1-\lambda_1)^{\mathrm{t}}(1-\lambda_2)^{\mathrm{t}}\right\}}{1-(1-\lambda_1)(1-\lambda_2)} \end{array} \right] \frac{2\sigma^4}{3\mathrm{n}} \end{aligned}\right\} \tag{13}$$

The lower control limit $\left(\mathrm{LCL_{(HEWMA)t}}\right)$ and upper control limit $\left(\mathrm{UCL_{(HEWMA)t}}\right)$ of the $\mathrm{HEWMA_{IM}}$ chart at the time i are respectively, given by

$$\left(\mathrm{UCL_{(HEWMA_{IM})i}}, \mathrm{LCL_{(HEWMA_{IM})i}}\right) = \sigma^2 \pm \mathrm{L}\sqrt{\mathrm{V}(\mathrm{HE_i})} \tag{14}$$

where the L is chart coefficient. It is determined in such a way that the IC, ARL of $\mathrm{HEWMA_{IM}}$ chart reaches a pre-specified desired level. The $\mathrm{HEWMA_{IM}}$ chart triggers an OOC signal whenever $\mathrm{HE_i}$ fall outside of the control limits $\left(\mathrm{UCL_{(HEWMA_{IM})i}}, \mathrm{LCL_{(HEWMA_{IM})i}}\right)$.

## 3 Performance Comparison Measurers

Quality experts employ various performance evaluation measures to assess the effectiveness of control charts. The average run length (ARL) is commonly used for comparison. In contrast, the extra quadratic loss (EQL), relative average run length (RARL), and performance comparison index (PCI) are employed to evaluate the overall performance of control charts. An algorithm is formulated within the R software to compute the numerical outcomes, and the Monte Carlo simulation technique is employed. Monte Carlo simulation with 20,000 iterations is executed at each shift ($\delta$), where $\delta = 1.00, 1.05, 1.10, 1.15, 1.20, 1.25, 1.35, 1.50, 1.75, 2.00, 2.50$ and $3.00$. The $\delta$ refers to a change in process mean over time or across samples. This $\delta$ is often measured in terms of $\sigma$ from the original process mean. The $\mathrm{HEWMA_{IM}}$ chart ARL findings on different $\delta$ and combination of $\lambda_1, \lambda_2$ are presented in Tables 1, 2, and 3, where the target $\mathrm{ARL_0} \cong 370$. RL

**Table 1** RL characteristics of the proposed control chart when n = 3 and $ARL_0 = 370$

| L | $\delta$ | 1.00 | 1.05 | 1.10 | 1.15 | 1.20 | 1.25 | 1.35 | 1.50 | 1.75 | 2.00 | 2.50 | 3.00 |
|---|---|---|---|---|---|---|---|---|---|---|---|---|---|
| $\lambda_1 = 0.05, \lambda_2 = 0.05$ | | | | | | | | | | | | | |
| 1.955 | ARL | 370.72 | 165.39 | 68.26 | 37.99 | 25.03 | 17.41 | 10.72 | 6.12 | 3.59 | 2.46 | 1.65 | 1.35 |
| | SDRL | 402.24 | 180.94 | 68.90 | 36.87 | 23.68 | 16.50 | 10.04 | 5.86 | 3.33 | 2.09 | 1.12 | 0.69 |
| | MDRL | 245.50 | 111.00 | 49.00 | 28.00 | 19.00 | 13.00 | 8.00 | 4.00 | 2.00 | 2.00 | 1.00 | 1.00 |
| $\lambda_1 = 0.05, \lambda_2 = 0.10$ | | | | | | | | | | | | | |
| 2.082 | ARL | 370.43 | 169.44 | 69.33 | 38.22 | 26.65 | 18.08 | 10.90 | 6.60 | 3.69 | 2.51 | 1.77 | 1.42 |
| | SDRL | 397.41 | 177.51 | 68.47 | 36.94 | 24.77 | 16.42 | 10.38 | 5.93 | 3.17 | 2.06 | 1.25 | 0.83 |
| | MDRL | 239.50 | 115.00 | 51.00 | 28.00 | 21.00 | 14.00 | 8.00 | 5.00 | 3.00 | 2.00 | 1.00 | 1.00 |
| $\lambda_1 = 0.05, \lambda_2 = 0.25$ | | | | | | | | | | | | | |
| 2.262 | ARL | 370.54 | 173.87 | 72.58 | 39.69 | 26.59 | 18.84 | 11.34 | 6.88 | 3.71 | 2.77 | 1.80 | 1.39 |
| | SDRL | 375.19 | 172.29 | 70.84 | 39.63 | 24.63 | 17.19 | 9.55 | 5.86 | 3.17 | 2.14 | 1.27 | 0.76 |
| | MDRL | 254.50 | 124.00 | 54.00 | 29.00 | 20.00 | 14.00 | 9.00 | 5.00 | 3.00 | 2.00 | 1.00 | 1.00 |
| $\lambda_1 = 0.05, \lambda_2 = 0.50$ | | | | | | | | | | | | | |
| 2.392 | ARL | 370.54 | 171.67 | 72.46 | 39.31 | 26.60 | 18.01 | 11.34 | 6.69 | 3.91 | 2.63 | 1.74 | 1.46 |
| | SDRL | 385.42 | 171.23 | 71.41 | 38.76 | 24.99 | 16.72 | 10.28 | 5.42 | 3.25 | 2.03 | 1.13 | 0.88 |
| | MDRL | 251.00 | 118.50 | 53.00 | 29.00 | 20.00 | 13.00 | 8.00 | 5.00 | 3.00 | 2.00 | 1.00 | 1.00 |
| $\lambda_1 = 0.10, \lambda_2 = 0.05$ | | | | | | | | | | | | | |
| 2.082 | ARL | 370.43 | 169.44 | 69.33 | 38.22 | 26.65 | 18.08 | 10.90 | 6.60 | 3.69 | 2.51 | 1.77 | 1.42 |
| | SDRL | 397.41 | 177.51 | 68.47 | 36.94 | 24.77 | 16.42 | 10.38 | 5.93 | 3.17 | 2.06 | 1.25 | 0.83 |
| | MDRL | 239.50 | 115.00 | 51.00 | 28.00 | 21.00 | 14.00 | 8.00 | 5.00 | 3.00 | 2.00 | 1.00 | 1.00 |
| $\lambda_1 = 0.10, \lambda_2 = 0.10$ | | | | | | | | | | | | | |
| 2.223 | ARL | 369.49 | 177.58 | 73.98 | 41.91 | 26.06 | 19.60 | 11.68 | 6.84 | 3.88 | 2.69 | 1.74 | 1.43 |
| | SDRL | 386.02 | 181.31 | 72.05 | 43.11 | 23.96 | 17.99 | 9.97 | 6.18 | 3.34 | 2.25 | 1.17 | 0.80 |
| | MDRL | 260.50 | 124.00 | 53.00 | 30.00 | 20.00 | 15.00 | 9.00 | 5.00 | 3.00 | 2.00 | 1.00 | 1.00 |
| $\lambda_1 = 0.10, \lambda_2 = 0.25$ | | | | | | | | | | | | | |
| 2.424 | ARL | 370.42 | 181.08 | 77.78 | 44.32 | 28.01 | 20.23 | 11.94 | 7.01 | 3.77 | 2.80 | 1.75 | 1.45 |
| | SDRL | 390.54 | 174.63 | 76.05 | 45.10 | 25.10 | 18.42 | 9.92 | 5.58 | 3.14 | 2.24 | 1.15 | 0.82 |
| | MDRL | 245.00 | 127.00 | 57.00 | 30.00 | 22.00 | 16.00 | 9.00 | 6.00 | 3.00 | 2.00 | 1.00 | 1.00 |
| $\lambda_1 = 0.10, \lambda_2 = 0.50$ | | | | | | | | | | | | | |
| 2.579 | ARL | 370.72 | 175.74 | 80.04 | 44.41 | 28.40 | 20.90 | 11.99 | 7.29 | 3.84 | 2.79 | 1.83 | 1.46 |
| | SDRL | 387.87 | 172.20 | 79.18 | 45.24 | 25.95 | 19.07 | 9.96 | 5.86 | 3.02 | 2.13 | 1.22 | 0.79 |
| | MDRL | 243.50 | 123.00 | 57.00 | 31.00 | 22.00 | 16.00 | 10.00 | 6.00 | 3.00 | 2.00 | 1.00 | 1.00 |
| $\lambda_1 = 0.25, \lambda_2 = 0.05$ | | | | | | | | | | | | | |
| 2.258 | ARL | 368.32 | 171.52 | 72.95 | 38.89 | 26.91 | 18.70 | 11.32 | 6.70 | 4.38 | 3.80 | 2.68 | 1.80 |
| | SDRL | 373.61 | 171.91 | 71.38 | 38.76 | 24.69 | 17.07 | 10.26 | 5.52 | 3.67 | 3.26 | 2.14 | 1.25 |
| | MDRL | 251.50 | 121.00 | 54.00 | 28.00 | 21.00 | 14.00 | 8.00 | 6.00 | 3.00 | 3.00 | 2.00 | 1.00 |
| $\lambda_1 = 0.25, \lambda_2 = 0.10$ | | | | | | | | | | | | | |
| 2.424 | ARL | 370.42 | 181.08 | 77.78 | 44.32 | 28.01 | 20.23 | 11.94 | 7.01 | 4.12 | 3.94 | 2.83 | 1.82 |
| | SDRL | 390.54 | 174.63 | 76.05 | 45.10 | 25.10 | 18.42 | 9.92 | 5.58 | 3.46 | 3.27 | 2.26 | 1.28 |
| | MDRL | 245.00 | 127.00 | 57.00 | 30.00 | 22.00 | 16.00 | 9.00 | 6.00 | 3.00 | 3.00 | 2.00 | 1.00 |
| $\lambda_1 = 0.25, \lambda_2 = 0.25$ | | | | | | | | | | | | | |
| 2.658 | ARL | 371.03 | 187.75 | 85.91 | 50.00 | 33.09 | 21.37 | 13.05 | 7.60 | 4.67 | 4.22 | 3.05 | 1.89 |

**Table 1** (continued)

| L | $\delta$ | 1.00 | 1.05 | 1.10 | 1.15 | 1.20 | 1.25 | 1.35 | 1.50 | 1.75 | 2.00 | 2.50 | 3.00 |
|---|---|---|---|---|---|---|---|---|---|---|---|---|---|
| | SDRL | 395.65 | 188.47 | 84.14 | 49.51 | 34.11 | 20.02 | 11.60 | 6.55 | 3.73 | 3.40 | 2.30 | 1.25 |
| | MDRL | 244.50 | 127.00 | 63.50 | 34.00 | 22.50 | 16.00 | 10.00 | 6.00 | 4.00 | 3.00 | 2.00 | 1.00 |
| $\lambda_1 = 0.25, \lambda_2 = 0.5$ | | | | | | | | | | | | | |
| 2.835 | ARL | 369.90 | 178.54 | 90.20 | 52.62 | 33.66 | 23.55 | 13.64 | 7.88 | 4.74 | 4.38 | 3.07 | 1.95 |
| | SDRL | 377.19 | 177.49 | 89.87 | 53.26 | 33.47 | 22.42 | 12.27 | 7.01 | 3.91 | 3.42 | 2.29 | 1.27 |
| | MDRL | 248.00 | 122.50 | 63.00 | 36.00 | 23.00 | 17.00 | 10.00 | 6.00 | 4.00 | 4.00 | 2.00 | 2.00 |
| $\lambda_1 = 0.5, \lambda_2 = 0.05$ | | | | | | | | | | | | | |
| 2.392 | ARL | 370.54 | 171.67 | 72.46 | 39.31 | 26.60 | 18.01 | 11.34 | 6.69 | 3.91 | 2.63 | 1.74 | 1.46 |
| | SDRL | 385.42 | 171.23 | 71.41 | 38.76 | 24.99 | 16.72 | 10.28 | 5.42 | 3.25 | 2.03 | 1.13 | 0.88 |
| | MDRL | 251.00 | 118.50 | 53.00 | 29.00 | 20.00 | 13.00 | 8.00 | 5.00 | 3.00 | 2.00 | 1.00 | 1.00 |
| $\lambda_1 = 0.5, \lambda_2 = 0.10$ | | | | | | | | | | | | | |
| 2.579 | ARL | 370.72 | 175.74 | 80.04 | 44.41 | 28.40 | 20.90 | 11.99 | 7.29 | 3.84 | 2.79 | 1.83 | 1.46 |
| | SDRL | 387.87 | 172.20 | 79.18 | 45.24 | 25.95 | 19.07 | 9.96 | 5.86 | 3.02 | 2.13 | 1.22 | 0.79 |
| | MDRL | 243.50 | 123.00 | 57.00 | 31.00 | 22.00 | 16.00 | 10.00 | 6.00 | 3.00 | 2.00 | 1.00 | 1.00 |
| $\lambda_1 = 0.5, \lambda_2 = 0.25$ | | | | | | | | | | | | | |
| 2.836 | ARL | 370.54 | 178.32 | 90.91 | 52.48 | 33.99 | 23.49 | 13.72 | 7.95 | 4.35 | 2.99 | 2.04 | 1.51 |
| | SDRL | 379.27 | 177.39 | 90.11 | 52.86 | 33.68 | 22.18 | 12.41 | 7.09 | 3.51 | 2.22 | 1.38 | 0.84 |
| | MDRL | 248.00 | 122.50 | 64.00 | 36.00 | 23.00 | 17.00 | 10.00 | 6.00 | 4.00 | 2.00 | 2.00 | 1.00 |
| $\lambda_1 = 0.5, \lambda_2 = 0.5$ | | | | | | | | | | | | | |
| 3.094 | ARL | 370.42 | 185.25 | 98.90 | 63.91 | 37.99 | 28.19 | 17.03 | 8.97 | 5.02 | 3.22 | 2.18 | 1.64 |
| | SDRL | 386.42 | 192.03 | 98.39 | 66.87 | 35.22 | 27.69 | 15.77 | 7.99 | 4.17 | 2.40 | 1.42 | 0.92 |
| | MDRL | 248.00 | 128.00 | 67.00 | 43.00 | 28.00 | 19.00 | 12.50 | 6.00 | 4.00 | 3.00 | 2.00 | 1.00 |

characteristics of the proposed chart at different sample sizes are also given in Table 1 when (n = 3), Table 2 (n = 6), and Table 3 (n = 9), where n is the sample size used in simulations. The details of these performance measures are given in the following subsections.

**Steps in Involved Algorithm**

In a simulation study, a sample of random data is generated in a manner that closely resembles a real-world scenario. The following steps are taken.

- To generate data which follows IM distribution.
- Ensure that the sample size, denoted as n, is fixed for each random sample.
- To obtain a random sample of size n, named as T from a gamma distribution with parameters $\left(3/2, 2\sigma_0^2\right)$, we can employ a random number generator.
- To obtain a sample with a Maxwell distribution, it is necessary to calculate the square root of T.
- To acquire a sample of size n from the random variable R, denoted as IM, we can make R equal to the reciprocal of x, i.e., R = 1/x.
- To calculate the $\text{HEWMA}_{\text{IM}}$ computing statistic, namely $E_i$ and $HE_i$, perform the following computations.

**Table 2** RL characteristics of the proposed control chart when n = 6 and $ARL_0 = 370$

| L | $\delta$ | 1.00 | 1.05 | 1.10 | 1.15 | 1.20 | 1.25 | 1.35 | 1.50 | 1.75 | 2.00 | 2.50 | 3.00 |
|---|---|---|---|---|---|---|---|---|---|---|---|---|---|
| $\lambda_1 = 0.05, \lambda_2 = 0.05$ | | | | | | | | | | | | | |
| 1.976 | ARL | 369.33 | 115.66 | 44.81 | 23.62 | 15.53 | 10.44 | 6.48 | 3.61 | 2.10 | 1.56 | 1.17 | 1.06 |
| | SDRL | 426.97 | 121.94 | 43.89 | 23.20 | 13.83 | 9.38 | 5.97 | 3.07 | 1.66 | 0.97 | 0.51 | 0.27 |
| | MDRL | 226.00 | 74.00 | 34.00 | 17.00 | 12.00 | 8.00 | 5.00 | 3.00 | 1.00 | 1.00 | 1.00 | 1.00 |
| $\lambda_1 = 0.05, \lambda_2 = 0.10$ | | | | | | | | | | | | | |
| 2.119 | ARL | 370.68 | 125.79 | 45.81 | 25.15 | 16.24 | 11.56 | 6.50 | 3.79 | 2.26 | 1.64 | 1.17 | 1.10 |
| | SDRL | 407.44 | 130.63 | 44.23 | 23.08 | 13.75 | 9.67 | 5.52 | 3.10 | 1.63 | 1.04 | 0.44 | 0.34 |
| | MDRL | 230.00 | 80.00 | 35.00 | 20.00 | 13.00 | 9.00 | 5.00 | 3.00 | 2.00 | 1.00 | 1.00 | 1.00 |
| $\lambda_1 = 0.05, \lambda_2 = 0.25$ | | | | | | | | | | | | | |
| 2.289 | ARL | 370.68 | 129.44 | 47.80 | 25.54 | 16.57 | 11.30 | 6.75 | 3.85 | 2.28 | 1.68 | 1.24 | 1.10 |
| | SDRL | 393.94 | 134.08 | 45.87 | 22.55 | 13.86 | 8.93 | 5.41 | 2.92 | 1.75 | 1.11 | 0.54 | 0.32 |
| | MDRL | 246.50 | 84.00 | 35.50 | 20.00 | 13.00 | 9.00 | 5.00 | 3.00 | 2.00 | 1.00 | 1.00 | 1.00 |
| $\lambda_1 = 0.05, \lambda_2 = 0.50$ | | | | | | | | | | | | | |
| 2.414 | ARL | 370.68 | 128.36 | 47.26 | 25.49 | 16.49 | 11.07 | 6.83 | 3.91 | 2.30 | 1.70 | 1.26 | 1.11 |
| | SDRL | 389.81 | 134.90 | 45.06 | 23.45 | 13.72 | 8.91 | 5.42 | 2.83 | 1.58 | 1.09 | 0.57 | 0.36 |
| | MDRL | 246.00 | 83.50 | 35.00 | 20.00 | 13.00 | 9.00 | 5.00 | 3.00 | 2.00 | 1.00 | 1.00 | 1.00 |
| $\lambda_1 = 0.10, \lambda_2 = 0.05$ | | | | | | | | | | | | | |
| 2.121 | ARL | 370.68 | 126.19 | 45.88 | 25.57 | 16.27 | 11.37 | 6.61 | 3.73 | 2.24 | 1.58 | 1.20 | 1.09 |
| | SDRL | 407.52 | 130.86 | 44.20 | 23.27 | 13.84 | 9.37 | 5.65 | 3.11 | 1.61 | 1.01 | 0.51 | 0.30 |
| | MDRL | 230.00 | 80.50 | 35.00 | 20.00 | 13.00 | 9.00 | 5.00 | 3.00 | 2.00 | 1.00 | 1.00 | 1.00 |
| $\lambda_1 = 0.10, \lambda_2 = 0.10$ | | | | | | | | | | | | | |
| 2.279 | ARL | 369.66 | 138.89 | 51.68 | 27.82 | 16.82 | 11.14 | 6.98 | 4.01 | 2.31 | 1.69 | 1.24 | 1.10 |
| | SDRL | 394.02 | 141.76 | 50.34 | 23.30 | 13.58 | 9.61 | 5.69 | 3.16 | 1.80 | 1.05 | 0.55 | 0.34 |
| | MDRL | 240.50 | 91.00 | 38.00 | 23.00 | 14.00 | 9.00 | 5.00 | 3.00 | 2.00 | 1.00 | 1.00 | 1.00 |
| $\lambda_1 = 0.10, \lambda_2 = 0.25$ | | | | | | | | | | | | | |
| 2.460 | ARL | 370.68 | 142.96 | 54.70 | 29.09 | 16.99 | 11.69 | 7.07 | 4.33 | 2.43 | 1.81 | 1.22 | 1.13 |
| | SDRL | 391.63 | 148.66 | 52.29 | 25.28 | 13.61 | 9.37 | 5.51 | 3.21 | 1.77 | 1.20 | 0.52 | 0.39 |
| | MDRL | 242.00 | 89.00 | 40.00 | 22.00 | 14.00 | 10.00 | 6.00 | 4.00 | 2.00 | 1.00 | 1.00 | 1.00 |
| $\lambda_1 = 0.10, \lambda_2 = 0.50$ | | | | | | | | | | | | | |
| 2.588 | ARL | 369.65 | 138.30 | 54.92 | 29.51 | 17.28 | 11.54 | 7.02 | 4.19 | 2.47 | 1.77 | 1.31 | 1.13 |
| | SDRL | 388.49 | 142.54 | 53.15 | 26.09 | 14.08 | 9.21 | 5.41 | 3.12 | 1.77 | 1.07 | 0.63 | 0.38 |
| | MDRL | 243.50 | 88.00 | 39.00 | 23.00 | 14.00 | 10.00 | 6.00 | 3.00 | 2.00 | 1.00 | 1.00 | 1.00 |
| $\lambda_1 = 0.25, \lambda_2 = 0.05$ | | | | | | | | | | | | | |
| 2.290 | ARL | 370.68 | 129.35 | 47.75 | 25.68 | 16.57 | 11.30 | 6.75 | 3.85 | 2.28 | 1.68 | 1.24 | 1.10 |
| | SDRL | 393.93 | 134.13 | 45.87 | 22.62 | 13.86 | 8.94 | 5.41 | 2.92 | 1.75 | 1.11 | 0.54 | 0.32 |
| | MDRL | 246.50 | 83.50 | 35.00 | 20.00 | 13.00 | 9.00 | 5.00 | 3.00 | 2.00 | 1.00 | 1.00 | 1.00 |
| $\lambda_1 = 0.25, \lambda_2 = 0.10$ | | | | | | | | | | | | | |
| 2.460 | ARL | 370.68 | 142.96 | 54.70 | 29.09 | 16.99 | 11.69 | 7.07 | 4.33 | 2.43 | 1.81 | 1.22 | 1.13 |
| | SDRL | 391.63 | 148.66 | 52.29 | 25.28 | 13.61 | 9.37 | 5.51 | 3.21 | 1.77 | 1.20 | 0.52 | 0.39 |
| | MDRL | 242.00 | 89.00 | 40.00 | 22.00 | 14.00 | 10.00 | 6.00 | 4.00 | 2.00 | 1.00 | 1.00 | 1.00 |
| $\lambda_1 = 0.25, \lambda_2 = 0.25$ | | | | | | | | | | | | | |
| 2.648 | ARL | 370.68 | 150.86 | 62.94 | 31.50 | 18.54 | 12.25 | 7.48 | 4.62 | 2.59 | 1.90 | 1.29 | 1.13 |

**Table 2** (continued)

| L | $\delta$ | 1.00 | 1.05 | 1.10 | 1.15 | 1.20 | 1.25 | 1.35 | 1.50 | 1.75 | 2.00 | 2.50 | 3.00 |
|---|---|---|---|---|---|---|---|---|---|---|---|---|---|
| | SDRL | 383.05 | 157.70 | 62.93 | 29.60 | 16.83 | 10.06 | 5.69 | 3.48 | 1.77 | 1.26 | 0.59 | 0.36 |
| | MDRL | 249.50 | 99.50 | 44.00 | 22.00 | 14.00 | 10.00 | 6.00 | 4.00 | 2.00 | 1.00 | 1.00 | 1.00 |
| $\lambda_1 = 0.25, \lambda_2 = 0.5$ | | | | | | | | | | | | | |
| 2.799 | ARL | 370.45 | 146.35 | 65.86 | 34.09 | 20.04 | 12.88 | 7.62 | 4.68 | 2.61 | 1.90 | 1.33 | 1.15 |
| | SDRL | 375.00 | 149.40 | 67.38 | 31.92 | 19.00 | 10.87 | 6.03 | 3.30 | 1.90 | 1.08 | 0.61 | 0.41 |
| | MDRL | 248.50 | 100.00 | 45.00 | 25.00 | 15.00 | 10.00 | 6.00 | 4.00 | 2.00 | 2.00 | 1.00 | 1.00 |
| $\lambda_1 = 0.5, \lambda_2 = 0.05$ | | | | | | | | | | | | | |
| 2.413 | ARL | 369.42 | 127.73 | 47.06 | 25.80 | 16.31 | 11.25 | 6.75 | 3.97 | 2.26 | 1.71 | 1.25 | 1.11 |
| | SDRL | 389.73 | 133.30 | 44.80 | 23.72 | 13.64 | 8.94 | 5.53 | 2.89 | 1.52 | 1.05 | 0.56 | 0.36 |
| | MDRL | 243.50 | 83.00 | 35.00 | 20.00 | 13.00 | 9.00 | 5.00 | 3.00 | 2.00 | 1.00 | 1.00 | 1.00 |
| $\lambda_1 = 0.5, \lambda_2 = 0.10$ | | | | | | | | | | | | | |
| 2.588 | ARL | 370.68 | 139.75 | 54.56 | 29.45 | 17.27 | 11.59 | 6.98 | 4.24 | 2.48 | 1.80 | 1.28 | 1.15 |
| | SDRL | 388.91 | 146.17 | 52.70 | 26.34 | 13.99 | 9.30 | 5.30 | 3.07 | 1.68 | 1.12 | 0.57 | 0.42 |
| | MDRL | 243.50 | 88.00 | 39.00 | 22.00 | 14.00 | 10.00 | 6.00 | 4.00 | 2.00 | 1.00 | 1.00 | 1.00 |
| $\lambda_1 = 0.5, \lambda_2 = 0.25$ | | | | | | | | | | | | | |
| 2.799 | ARL | 369.17 | 146.09 | 65.44 | 34.40 | 19.79 | 12.81 | 7.61 | 4.78 | 2.58 | 1.89 | 1.34 | 1.11 |
| | SDRL | 371.13 | 149.42 | 66.55 | 32.37 | 18.99 | 10.89 | 5.87 | 3.56 | 1.81 | 1.17 | 0.63 | 0.34 |
| | MDRL | 249.00 | 99.50 | 45.00 | 25.00 | 15.00 | 10.00 | 6.00 | 4.00 | 2.00 | 1.00 | 1.00 | 1.00 |
| $\lambda_1 = 0.5, \lambda_2 = 0.5$ | | | | | | | | | | | | | |
| 2.994 | ARL | 370.28 | 151.26 | 76.87 | 38.52 | 23.87 | 16.09 | 8.80 | 4.83 | 2.79 | 2.01 | 1.34 | 1.64 |
| | SDRL | 367.15 | 152.22 | 77.84 | 38.23 | 22.35 | 14.77 | 7.65 | 3.93 | 2.03 | 1.25 | 0.62 | 0.92 |
| | MDRL | 278.00 | 108.00 | 51.00 | 26.00 | 16.00 | 11.00 | 7.00 | 4.00 | 2.00 | 2.00 | 1.00 | 1.00 |

- The initial five procedures should be repeated until the desired number of subgroups are achieved.
- The control limits will be established according to the methodology outlined in the preceding section.
- Plotting all values of the $HE_i$ statistic in relation to the control limits.

### 3.1 The ARL Measure

The use of ARL to identify the flaws in the production process is a common comparison criterion for gauging the effectiveness of control charts. As the process means altered, it is taken into account from the measurement values frequency, which is outside of our control. A control chart, which catches the changes earlier, is more effective since it instantly detects the anomaly of the production process, allowing the cause inquiry and solution to be handled immediately. The ARL is defined as the average number of sample points plotted until the first OOC signal is detected. The target $ARL_0$ is achieved through the developed algorithms to detect the shifts rapidly and reliably. The ARL is categorized as IC $ARL(ARL_0)$ and OOC $ARL(ARL_1)$. If the process is IC state, the $ARL_0$ needs to be large

**Table 3** RL characteristics of the proposed control chart when n = 9 and $ARL_0 = 370$

| L | $\delta$ | 1.00 | 1.05 | 1.10 | 1.15 | 1.20 | 1.25 | 1.35 | 1.50 | 1.75 | 2.00 | 2.50 | 3.00 |
|---|---|---|---|---|---|---|---|---|---|---|---|---|---|
| $\lambda_1 = 0.05, \lambda_2 = 0.05$ | | | | | | | | | | | | | |
| 1.949 | ARL | 369.40 | 86.11 | 30.44 | 16.11 | 10.19 | 7.31 | 4.58 | 2.62 | 1.62 | 1.27 | 1.07 | 1.01 |
| | SDRL | 416.87 | 86.43 | 27.80 | 14.95 | 9.22 | 6.40 | 4.09 | 2.19 | 1.08 | 0.60 | 0.27 | 0.10 |
| | MDRL | 222.50 | 64.00 | 24.00 | 12.00 | 8.00 | 6.00 | 3.00 | 2.00 | 1.00 | 1.00 | 1.00 | 1.00 |
| $\lambda_1 = 0.05, \lambda_2 = 0.10$ | | | | | | | | | | | | | |
| 2.091 | ARL | 369.44 | 90.74 | 33.14 | 16.86 | 10.96 | 8.16 | 4.59 | 2.69 | 1.70 | 1.33 | 1.08 | 1.02 |
| | SDRL | 409.00 | 88.19 | 29.05 | 14.88 | 9.00 | 7.10 | 3.80 | 2.10 | 1.11 | 0.65 | 0.28 | 0.12 |
| | MDRL | 235.00 | 68.00 | 26.00 | 14.00 | 9.00 | 6.00 | 4.00 | 2.00 | 1.00 | 1.00 | 1.00 | 1.00 |
| $\lambda_1 = 0.05, \lambda_2 = 0.25$ | | | | | | | | | | | | | |
| 2.267 | ARL | 371.55 | 92.66 | 33.91 | 17.49 | 11.74 | 7.90 | 4.98 | 2.74 | 1.79 | 1.33 | 1.09 | 1.02 |
| | SDRL | 404.18 | 90.51 | 29.61 | 15.08 | 9.43 | 6.37 | 3.86 | 2.00 | 1.15 | 0.67 | 0.31 | 0.13 |
| | MDRL | 260.00 | 68.00 | 27.00 | 15.00 | 10.00 | 6.00 | 4.00 | 2.00 | 1.00 | 1.00 | 1.00 | 1.00 |
| $\lambda_1 = 0.05, \lambda_2 = 0.50$ | | | | | | | | | | | | | |
| 2.385 | ARL | 369.61 | 94.35 | 33.91 | 17.11 | 11.52 | 7.95 | 4.90 | 2.85 | 1.71 | 1.39 | 1.11 | 1.03 |
| | SDRL | 384.51 | 90.44 | 29.81 | 14.33 | 9.28 | 6.44 | 3.73 | 1.95 | 1.02 | 0.71 | 0.35 | 0.17 |
| | MDRL | 259.00 | 68.00 | 27.00 | 14.00 | 9.00 | 7.00 | 4.00 | 2.00 | 1.00 | 1.00 | 1.00 | 1.00 |
| $\lambda_1 = 0.10, \lambda_2 = 0.05$ | | | | | | | | | | | | | |
| 2.091 | ARL | 369.44 | 90.74 | 33.14 | 16.86 | 10.96 | 8.16 | 4.59 | 2.69 | 1.70 | 1.33 | 1.08 | 1.02 |
| | SDRL | 409.00 | 88.19 | 29.05 | 14.88 | 9.00 | 7.10 | 3.80 | 2.10 | 1.11 | 0.65 | 0.28 | 0.12 |
| | MDRL | 235.00 | 68.00 | 26.00 | 14.00 | 9.00 | 6.00 | 4.00 | 2.00 | 1.00 | 1.00 | 1.00 | 1.00 |
| $\lambda_1 = 0.10, \lambda_2 = 0.10$ | | | | | | | | | | | | | |
| 2.240 | ARL | 369.61 | 96.99 | 34.74 | 17.94 | 12.11 | 8.42 | 4.82 | 2.95 | 1.72 | 1.31 | 1.09 | 1.03 |
| | SDRL | 385.49 | 98.54 | 31.35 | 15.18 | 10.29 | 6.46 | 3.75 | 2.27 | 1.05 | 0.65 | 0.32 | 0.18 |
| | MDRL | 264.50 | 69.00 | 27.00 | 15.00 | 10.00 | 7.00 | 4.00 | 2.00 | 1.00 | 1.00 | 1.00 | 1.00 |
| $\lambda_1 = 0.10, \lambda_2 = 0.25$ | | | | | | | | | | | | | |
| 2.437 | ARL | 369.61 | 111.20 | 37.52 | 20.20 | 12.23 | 8.55 | 5.25 | 3.06 | 1.87 | 1.39 | 1.11 | 1.03 |
| | SDRL | 371.47 | 109.61 | 33.27 | 17.64 | 9.36 | 6.71 | 4.13 | 2.26 | 1.24 | 0.72 | 0.36 | 0.17 |
| | MDRL | 264.00 | 80.00 | 29.00 | 16.00 | 10.50 | 7.00 | 4.00 | 2.00 | 1.00 | 1.00 | 1.00 | 1.00 |
| $\lambda_1 = 0.10, \lambda_2 = 0.50$ | | | | | | | | | | | | | |
| 2.568 | ARL | 370.44 | 109.37 | 38.10 | 20.63 | 12.36 | 8.53 | 5.33 | 3.10 | 1.88 | 1.43 | 1.11 | 1.04 |
| | SDRL | 378.34 | 112.36 | 34.10 | 18.38 | 9.84 | 6.85 | 4.02 | 2.22 | 1.18 | 0.75 | 0.33 | 0.19 |
| | MDRL | 253.00 | 77.50 | 28.50 | 16.00 | 10.00 | 7.00 | 4.00 | 3.00 | 1.00 | 1.00 | 1.00 | 1.00 |
| $\lambda_1 = 0.25, \lambda_2 = 0.05$ | | | | | | | | | | | | | |
| 2.266 | ARL | 370.19 | 93.38 | 33.93 | 17.14 | 11.84 | 7.96 | 4.98 | 2.80 | 1.70 | 1.36 | 1.10 | 1.03 |
| | SDRL | 400.55 | 90.88 | 29.53 | 14.87 | 9.50 | 6.47 | 3.86 | 2.06 | 1.04 | 0.71 | 0.34 | 0.16 |
| | MDRL | 259.50 | 69.00 | 27.00 | 14.00 | 10.00 | 6.00 | 4.00 | 2.00 | 1.00 | 1.00 | 1.00 | 1.00 |
| $\lambda_1 = 0.25, \lambda_2 = 0.10$ | | | | | | | | | | | | | |
| 2.437 | ARL | 369.61 | 111.20 | 37.52 | 20.20 | 12.23 | 8.55 | 5.25 | 3.06 | 1.87 | 1.39 | 1.11 | 1.03 |
| | SDRL | 371.47 | 109.61 | 33.27 | 17.64 | 9.36 | 6.71 | 4.13 | 2.26 | 1.24 | 0.72 | 0.36 | 0.17 |
| | MDRL | 264.00 | 80.00 | 29.00 | 16.00 | 10.50 | 7.00 | 4.00 | 2.00 | 1.00 | 1.00 | 1.00 | 1.00 |
| $\lambda_1 = 0.25, \lambda_2 = 0.25$ | | | | | | | | | | | | | |
| 2.628 | ARL | 370.44 | 122.59 | 45.23 | 21.96 | 13.39 | 9.42 | 5.10 | 3.12 | 1.96 | 1.42 | 1.13 | 1.03 |

**Table 3** (continued)

| L | $\delta$ | 1.00 | 1.05 | 1.10 | 1.15 | 1.20 | 1.25 | 1.35 | 1.50 | 1.75 | 2.00 | 2.50 | 3.00 |
|---|---|---|---|---|---|---|---|---|---|---|---|---|---|
| | SDRL | 388.83 | 121.63 | 44.69 | 19.49 | 11.53 | 7.15 | 3.80 | 2.11 | 1.21 | 0.73 | 0.38 | 0.18 |
| | MDRL | 247.50 | 87.00 | 32.00 | 16.00 | 11.00 | 8.00 | 4.00 | 3.00 | 2.00 | 1.00 | 1.00 | 1.00 |
| $\lambda_1 = 0.25, \lambda_2 = 0.5$ | | | | | | | | | | | | | |
| 2.793 | ARL | 370.19 | 127.43 | 51.00 | 23.95 | 14.29 | 9.66 | 5.58 | 3.38 | 2.04 | 1.51 | 1.16 | 1.04 |
| | SDRL | 372.67 | 123.91 | 51.66 | 22.07 | 12.15 | 7.99 | 4.21 | 2.22 | 1.20 | 0.80 | 0.41 | 0.20 |
| | MDRL | 259.00 | 90.00 | 36.00 | 17.00 | 11.00 | 8.00 | 5.00 | 3.00 | 2.00 | 1.00 | 1.00 | 1.00 |
| $\lambda_1 = 0.5, \lambda_2 = 0.05$ | | | | | | | | | | | | | |
| 2.385 | ARL | 369.61 | 94.35 | 33.91 | 17.11 | 11.52 | 7.95 | 4.90 | 2.85 | 1.71 | 1.39 | 1.11 | 1.03 |
| | SDRL | 384.51 | 90.44 | 29.81 | 14.33 | 9.28 | 6.44 | 3.73 | 1.95 | 1.02 | 0.71 | 0.35 | 0.17 |
| | MDRL | 259.00 | 68.00 | 27.00 | 14.00 | 9.00 | 7.00 | 4.00 | 2.00 | 1.00 | 1.00 | 1.00 | 1.00 |
| $\lambda_1 = 0.5, \lambda_2 = 0.10$ | | | | | | | | | | | | | |
| 2.569 | ARL | 370.44 | 109.53 | 37.98 | 20.65 | 12.37 | 8.54 | 5.32 | 3.12 | 1.88 | 1.44 | 1.11 | 1.04 |
| | SDRL | 378.34 | 112.33 | 33.90 | 18.38 | 9.83 | 6.87 | 4.02 | 2.22 | 1.19 | 0.75 | 0.34 | 0.19 |
| | MDRL | 253.00 | 78.00 | 28.50 | 16.00 | 10.00 | 7.00 | 4.00 | 3.00 | 1.00 | 1.00 | 1.00 | 1.00 |
| $\lambda_1 = 0.5, \lambda_2 = 0.25$ | | | | | | | | | | | | | |
| 2.793 | ARL | 370.19 | 127.43 | 51.00 | 23.95 | 14.29 | 9.66 | 5.58 | 3.38 | 2.04 | 1.51 | 1.16 | 1.04 |
| | SDRL | 372.67 | 123.91 | 51.66 | 22.07 | 12.15 | 7.99 | 4.21 | 2.22 | 1.20 | 0.80 | 0.41 | 0.20 |
| | MDRL | 259.00 | 90.00 | 36.00 | 17.00 | 11.00 | 8.00 | 5.00 | 3.00 | 2.00 | 1.00 | 1.00 | 1.00 |
| $\lambda_1 = 0.5, \lambda_2 = 0.5$ | | | | | | | | | | | | | |
| 2.950 | ARL | 370.47 | 127.59 | 58.14 | 28.94 | 16.48 | 11.27 | 6.00 | 3.51 | 2.08 | 1.52 | 1.17 | 1.05 |
| | SDRL | 386.65 | 125.71 | 61.45 | 27.87 | 15.80 | 10.22 | 4.48 | 2.39 | 1.22 | 0.77 | 0.42 | 0.23 |
| | MDRL | 259.00 | 91.00 | 38.50 | 20.00 | 12.00 | 8.00 | 5.00 | 3.00 | 2.00 | 1.00 | 1.00 | 1.00 |

enough to avoid frequent false alarms. If a shift is detected by a algorithm even though there was no such shift occurred in the process, that is referred to false alarm [26]. However, $ARL_1$ should be small enough to quickly detect the shift(s) in the process parameters. It is necessary for the better performance of the control chart that it should have a smaller $ARL_1$ with a fixed $ARL_0$ at the desired level. This study used MC simulation to determine ARLs, since it's a straightforward method comparable in reliability and accuracy to other methods [2, 50, 72].

$$\mathrm{ARL} = \frac{1}{1 - \mathrm{P}\left[\mathrm{LCL} \le HE_i \le \mathrm{UCL}\right]}$$

or

$$\mathrm{ARL} = \frac{\sum_{t=1}^{N} \mathrm{RL_t}}{\mathrm{N}}$$

where $RL_t$ is the simulation of $t_{th}$ round, which is observed before the 1st sample gose out of control limits, and N is the number of repetitions.

### 3.2 Overall Performance Measures

The EQL, RARL, and PCI performance evaluation measures are calculated to measure a control chart's overall effectiveness. The following subsections provide more details on these measures.

#### 3.2.1 Extra Quadratic Loss

EQL is defined as a weighted ARL of shift domain ($\delta_{\min} < \delta < \delta_{\max}$), where shift's square is used as a weight, that is mathematically written as,

$$\text{EQL} = \frac{1}{\delta_{\max} - \delta_{\min}} \int_{\delta_{\min}}^{\delta_{\max}} \delta^2 \text{ARL}(\delta) \text{d}\delta$$

The maximum and minimum of $\delta$ are $\delta_{\max}$ and $\delta_{\min}$, where ARL($\delta$) is an ARL of a specific chart at $\delta$. A control chart with a minimum EQL value is considered superior in performance [35–37].

#### 3.2.2 Relative Average Run Length

RARL can be described as the average fraction between ARL($\delta$) and benchmark chart, where ARL($\delta$) is ARL of a specific chart.

$$\text{RARL} = \frac{1}{\delta_{\max} - \delta_{\min}} \int_{\delta_{\min}}^{\delta_{\max}} \frac{\text{ARL}(\delta)}{\text{ARL}_{\text{benchmark}}(\delta)} \text{d}\delta$$

The benchmark chart is defined as taking the lowest EQL value. The chart with the least RARL value is considered a better chart.

#### 3.2.3 Performance Comparison Index

PCI is the ratio of the EQL of a specific chart to the EQL of the benchmark (BMC) chart. It can be stated as

$$\text{PCI} = \frac{\text{EQL}}{\text{EQL}_{\text{BMC}}}$$

A chart is preferred over the other charts with a minimum, PCI value [41].

## 4 Comparative Study

In this section, we discussed the performance of the proposed chart by choosing the values for $\lambda_1$ and $\lambda_2$ (the smoothing parameter for the $\text{HEWMA}_{\text{IM}}$ chart, which is crucial as it directly influences the sensitivity and responsiveness of the chart to process shifts. Typically, the chart is more sensitive to minor shifts when the weight of

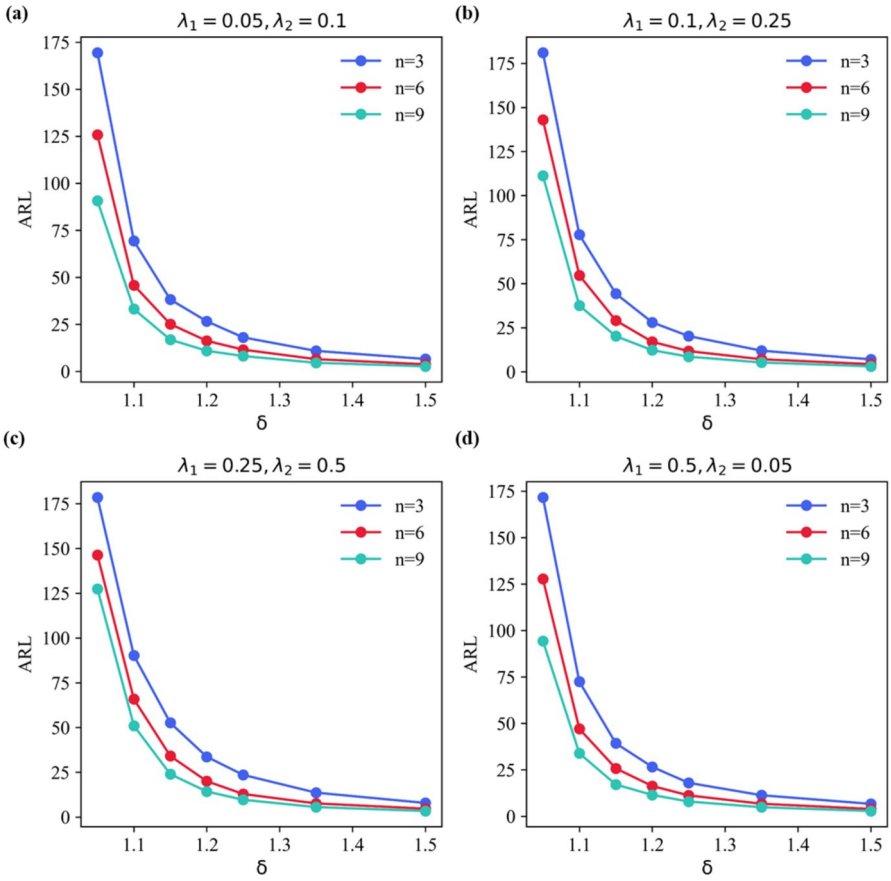


**Fig. 1** ARLs comparison of the proposed $\text{HEWMA}_{\text{IM}}$ chart when $n = (3, 6, 9)$. **a** at $\lambda_1 = 0.05$ and $\lambda_2 = 0.1$, **b** $\lambda_1 = 0.1$ and $\lambda_2 = 0.25$, **c** $\lambda_1 = 0.25$ and $\lambda_2 = 0.5$ and **d** $\lambda_1 = 0.5$ and $\lambda_2 = 0.05$

more recent observations is increased by lower values of $\lambda_1$ and $\lambda_2$ while the impact of recent observations is reduced by higher values, resulting in a delayed signal time but greater stability in the presence of noise. The performance of the $\text{HEWMA}_{\text{IM}}$ chart is assessed on various combinations of $\lambda_1$ and $\lambda_2$. For example, in the case of small smoothing constants $\lambda_1 = 0.05$ and $\lambda_2 = 0.10$, $\text{HEWMA}_{\text{IM}}$ charts respond quickly to shifts ($\delta = 1.05$ to 1.15) as observed by the rapid decrease in ARL values (e.g., for $n = 3$, ARL drops from 169.44 to 38.22 for $\delta = 1.05\&1.15$), see Fig. 1a. In case of other combinations ($\lambda_1 = 0.10$ and $\lambda_2 = 0.25$), the ARL values shown in the $\text{HEWMA}_{\text{IM}}$ chart for $\delta = 1.10$ is 77.78 at $n = 3$ which is larger as compared to the smaller $\lambda$ but still efficient for detecting shifts, see Fig. 1b. This provides a tradeoff between early detection and robustness to noise. As we increase the size of the smoothing parameter $\lambda_1 = 0.25$ and $\lambda_2 = 0.50$, $\text{HEWMA}_{\text{IM}}$ chart becomes more resistant but slower to detect smaller shifts, however as $\delta$ size increases the performance improves significantly, see Fig. 1c and d.

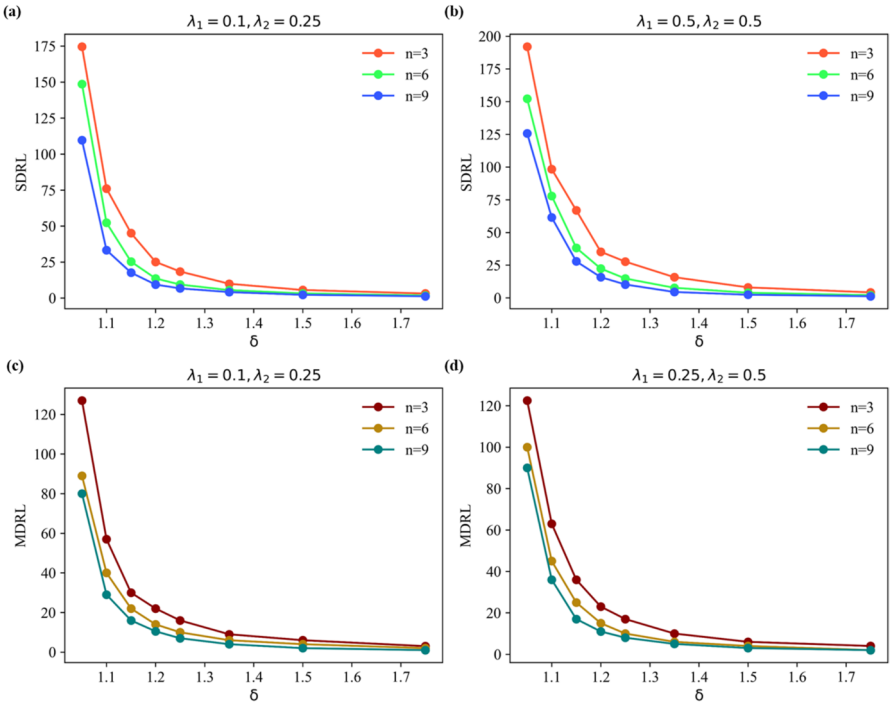


**Fig. 2** Comparison of the proposed $\text{HEWMA}_{\text{IM}}$ chart when $n = (3, 6, 9)$. **a** SDRL at $\lambda_1 = 0.1$ and $\lambda_2 = 0.25$, **b** SDRL at $\lambda_1 = 0.5$ and $\lambda_2 = 0.5$, **c** MDRL at $\lambda_1 = 0.1$ and $\lambda_2 = 0.25$ and **d** MDRL at $\lambda_1 = 0.25$ and $\lambda_2 = 0.5$

$\text{HEWMA}_{\text{IM}}$ chart with smaller $\lambda$ values is most effective in detecting small shifts, with lower ARL values compared to the larger $\lambda$ combinations. As the shift size increases to 1.10 or 1.15, the difference in ARL between the smaller and larger $\lambda$ values decrease. From the comparison of ARL, SDRL, and MDRL, it can be observed that for larger shifts, the performance of the proposed chart with different $\lambda$ combinations converge. For all $\lambda$ combinations, as the sample size increases from 3, 6 to 9, the ARL, SDRL and MDRL values decrease, indicating faster detection of shifts with larger sample sizes, for ARL see Fig. 1a–d and SDRL and MDRL, see Fig. 2a–d. The results suggest that larger sample sizes provide better sensitivity for detecting both small and large shifts, regardless of $\lambda$ selection.

The analysis of different combinations of $\lambda_1$ and $\lambda_2$ for $\text{HEWMA}_{\text{IM}}$ chart reveals the impact that these parameters have on the chart's ability to detect shifts in process behavior. At $(\lambda_1, \lambda_2 = 0.05)$ for small ($\delta = 1.05$ to 1.15) the ARL values are generally low, indicating a quick response, particularly for $n = 3$ (e.g., ARL = 37.99, for $\delta = 1.15$), see Fig. 3a. For $\delta > 1.50$ are also detected effectively, with ARL values as low as $n = 6$ for $\delta = 1.50$ with $n = 3$. The combination of $(\lambda_1, \lambda_2 = 0.10)$ offers a slightly lower detection compared to $\lambda = 0.05$ with higher ARL values (e.g., ARL = 41.91 for $\delta = 1.15$), see Fig. 3b. This setting provides a balanced sensitivity

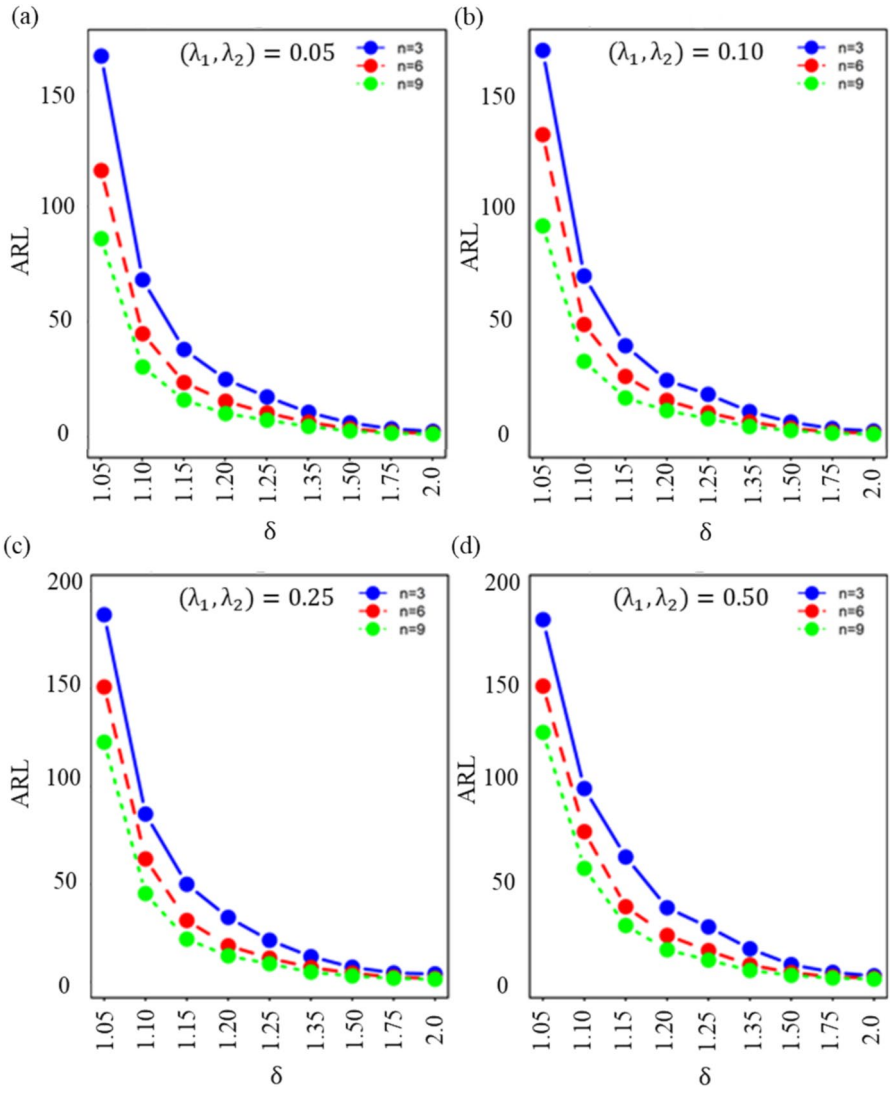


**Fig. 3** ARLs comparison of the proposed $\text{HEWMA}_{\text{IM}}$ chart when n = (3, 6, 9) (**a**) at $(\lambda_1, \lambda_2) = 0.05$ (**b**) at $(\lambda_1, \lambda_2) = 0.10$ (**c**) at $(\lambda_1, \lambda_2) = 0.25$ and (**d**) at $(\lambda_1, \lambda_2) = 0.50$

for detecting both small and large shifts. When $(\lambda_1, \lambda_2 = 0.25)$ for large shifts detection speeds are still competitive with ARLs between 7 and 9 for $\boldsymbol{\delta} = 1.50$ across different sample sizes, see Fig. 3c. For $(\lambda_1, \lambda_2 = 0.50)$ the $\text{HEWMA}_{\text{IM}}$ chart indicating that ARL values are competitive but slightly slower (e.g., ARL = 8.97 for $\boldsymbol{\delta} = 1.50$, n = 3) indicating this combination prioritizes resistance and less responsive to smaller changes, see Fig. 3d.

With same $\lambda$ $(\lambda_1 = \lambda_2)$ the proposed chart is less sensitive to small shifts, particularly as $\lambda$ value increase. For instance, when $\lambda_1 = 0.5$, and $\lambda_2 = 0.5$, the ARL values

**Table 4** RL characteristics of the $V_{1M}$ control chart when n = 3, 6, 9 and $ARL_0 = 370$

| δ | n = 3 | | | n = 6 | | | n = 9 | | |
|---|---|---|---|---|---|---|---|---|---|
| | ARL | SDRL | MDRL | ARL | SDRL | MDRL | ARL | SDRL | MDRL |
| $V_{1M}$ | | | | | | | | | |
| 1.00 | 370.54 | 369.09 | 258.00 | 369.3 | 368.14 | 257.00 | 369.84 | 369.24 | 254.00 |
| 1.25 | 96.10 | 93.95 | 67.00 | 60.41 | 60.35 | 42.00 | 39.38 | 39.15 | 27.00 |
| 1.50 | 28.75 | 28.24 | 20.00 | 14.48 | 14.02 | 10.00 | 8.15 | 7.71 | 6.00 |
| 1.75 | 12.74 | 12.14 | 9.00 | 6.05 | 5.53 | 4.00 | 3.32 | 2.68 | 2.00 |
| 2.00 | 7.38 | 6.80 | 5.00 | 3.34 | 2.82 | 2.00 | 2.03 | 1.44 | 1.00 |
| 2.25 | 4.72 | 4.13 | 3.00 | 2.32 | 1.76 | 2.00 | 1.49 | 0.83 | 1.00 |
| 2.50 | 3.48 | 2.95 | 3.00 | 1.83 | 1.22 | 1.00 | 1.25 | 0.57 | 1.00 |
| 2.75 | 2.78 | 2.18 | 2.00 | 1.53 | 0.91 | 1.00 | 1.14 | 0.4 | 1.00 |
| 3.00 | 2.33 | 1.70 | 2.00 | 1.34 | 0.69 | 1.00 | 1.09 | 0.28 | 1.00 |
| 5.00 | 1.25 | 0.58 | 1.00 | 1.04 | 0.16 | 1.00 | 1.01 | 0.03 | 1.00 |

are higher, indicating slower detection e.g., ARL = 63.91 for $\delta = 1.15$, n = 3. When different $\lambda_1, \lambda_2$ values are used, the chart is generally more sensitive to small shifts compared to when $\lambda_1 = \lambda_2$. For example, when $\lambda_1 = 0.5, \lambda_2 = 0.05$ the ARL value is 39.31 at the same shift and sample size. For moderate and large shifts, using different $\lambda$ values also result in faster detection compared to same $\lambda$ values. For example, ARL = 6.50 for $\delta = 1.50$ with $\lambda_1 = 0.05$, $\lambda_2 = 0.10$ and n = 3 compared to ARL = 8.97 for same $\lambda_1 = \lambda_2 = 0.50$. Overall, different $\lambda_1, \lambda_2$ provide faster detection for small and large shifts, making them more effective in real-life scenarios where early detection is critical. Where same ($\lambda_1 = \lambda_2$) are more stable for processes with moderate changes but may be slower for small shifts.

As comparing the proposed $HEWMA_{IM}$ chart to the $V_{IM}$, $EWMA_{IM}$ and $EEWMA_{IM}$ charts. The assessments are based on the ARL, EQL, RARL, and PCI measures. It can be observed that the ARL values of $HEWMA_{IM}$ chart are smaller than the ARL values of the $V_{IM}$, $EWMA_{IM}$ and $EEWMA_{IM}$ charts (see Tables 1, 2, 3, 4, 5, and 6). For example, at n = 3, $\delta = 1.25$, 1.50, and $ARL_0 = 370$, the ARL values of $HEWMA_{IM}$, $V_{IM}$ and $EWMA_{IM}$ charts are (17.41,6.12), (96.10,28.75), and (38.11,10.37), respectively (see Tables 1, 4, and 5). Similarly, at n = 9, $\delta = 1.25$, and $ARL_0 = 370$, the ARL values of $HEWMA_{IM}$, $V_{IM}$ and $EWMA_{IM}$ chart is 7.31, 39.38, and 12.98, respectively (see Tables 3, 4 and 5). This shows that the $HEWMA_{IM}$ chart is more sensitive in detecting a shift than competing charts. It is observed that as the smoothing constant $\lambda$ decreases, the performance of the proposed $HEWMA_{IM}$ chart increases.

It is worth mentioning that as the size of the shifts increases, the ARL values of the proposed $HEWMA_{IM}$ chart reduce significantly as compared to the $V_{IM}$ and $EWMA_{IM}$ charts. As an illustration, at n = 9, $\delta = 1.25$, and $ARL_0 = 370$ the ARL values of $HEWMA_{IM}$, $V_{IM}$ and $EWMA_{IM}$ charts are 7.31, 39.38, and 12.98, respectively. The MDRL and SDRL exhibited the same behavior as the ARL. Figure 4 depicts the significance of the proposed chart.

**Table 5** RL characteristics of the $EWMA_{IM}$ control chart when n = 3, 6, 9, $\lambda = 0.5$ and $ARL_0 = 370$

| δ | n = 3 | | | n = 6 | | | n = 9 | | |
|---|---|---|---|---|---|---|---|---|---|
| | ARL | SDRL | MDRL | ARL | SDRL | MDRL | ARL | SDRL | MDRL |
| $EWMA_{IM}$ | | | | | | | | | |
| 1.00 | 371.40 | 374.38 | 260.00 | 374.13 | 375.80 | 259.00 | 370.24 | 369.91 | 256.00 |
| 1.05 | 211.91 | 212.66 | 148.00 | 175.38 | 174.48 | 122.00 | 148.47 | 149.10 | 103.00 |
| 1.10 | 127.44 | 126.59 | 89.00 | 88.65 | 89.80 | 61.00 | 69.50 | 69.47 | 48.00 |
| 1.15 | 81.60 | 82.49 | 57.00 | 50.73 | 50.14 | 35.00 | 35.77 | 36.78 | 25.00 |
| 1.20 | 55.43 | 56.34 | 38.00 | 30.66 | 31.15 | 21.00 | 20.54 | 21.15 | 14.00 |
| 1.25 | 38.11 | 38.43 | 26.00 | 20.09 | 20.57 | 14.00 | 12.98 | 13.38 | 9.00 |
| 1.35 | 21.29 | 21.69 | 14.00 | 9.82 | 10.01 | 7.00 | 5.83 | 6.18 | 4.00 |
| 1.50 | 10.37 | 10.73 | 7.00 | 4.27 | 4.53 | 2.00 | 2.39 | 2.55 | 1.00 |
| 1.75 | 4.44 | 4.75 | 3.00 | 1.68 | 1.60 | 1.00 | 1.14 | 0.57 | 1.00 |
| 2 | 2.35 | 2.40 | 1.00 | 1.14 | 0.54 | 1.00 | 1.00 | 0.11 | 1.00 |

**Table 6** RL characteristics of the $EEWMA_{IM}$ control chart when n = 3, 6, 9 and $ARL_0 = 370$

| $\delta$ | $\lambda = 0.1, 0.05$ | | | $\lambda = 0.25, 0.1$ | | |
|---|---|---|---|---|---|---|
| | n = 3 | n = 6 | n = 9 | n = 3 | n = 6 | n = 9 |
| $EEWMA_{IM}$ | | | | | | |
| 1.25 | 28.13 | 21.21 | 18.41 | 27.28 | 18.14 | 14.82 |
| 1.50 | 22.26 | 9.53 | 8.43 | 10.99 | 7.85 | 6.71 |
| 1.75 | 7.41 | 5.75 | 5.11 | 6.64 | 4.90 | 4.21 |
| 2.00 | 5.13 | 4.01 | 3.54 | 4.73 | 3.52 | 3.41 |
| 2.25 | 3.91 | 3.02 | 2.68 | 3.63 | 2.73 | 2.36 |
| 2.50 | 3.18 | 2.44 | 2.11 | 2.99 | 2.25 | 1.91 |
| 2.75 | 2.61 | 2.02 | 1.87 | 2.52 | 1.91 | 1.65 |
| 3 | 2.33 | 1.84 | 1.56 | 2.23 | 1.67 | 1.51 |
| 5 | 1.32 | 1.17 | 1.05 | 1.31 | 1.07 | 1.04 |

In Fig. 4a the ARL comparison of $HEWMA_{IM}$ chart when $\lambda = (0.05, 0.10, 0.25 \text{ and } 0.50)$ with existing $EWMA_{IM}(\lambda = 0.50)$, $V_{IM}$ and $EEWMA_{IM}(\lambda = 0.25, 0.10)$ chart proved the efficiency of the proposed chart on existing charts. Where the median run length comparison also yielded similar results to the proposed chart on existing charts, see Fig. 4b. Furthermore, we compared the proposed chart versus competitive charts using EQL, RARL, and PCI. Table 7 highlighted that the proposed $HEWMA_{IM}$ chart outperformed the $V_{IM}$, and $EWMA_{IM}$ charts in terms of overall performance at sample size n = 3,6 and 9. For example, at n = 6 and $ARL_0 = 370$, the EQL, RARL, and PCI values of the $HEWMA_{IM}$(55.39, 1.00, 1.00) are lesser than the EQL, RARL, and PCI values of the $V_{IM}$(58.87, 1.06, 1.11) and $EWMA_{IM}$(58.87, 1.06, 1.11) charts.

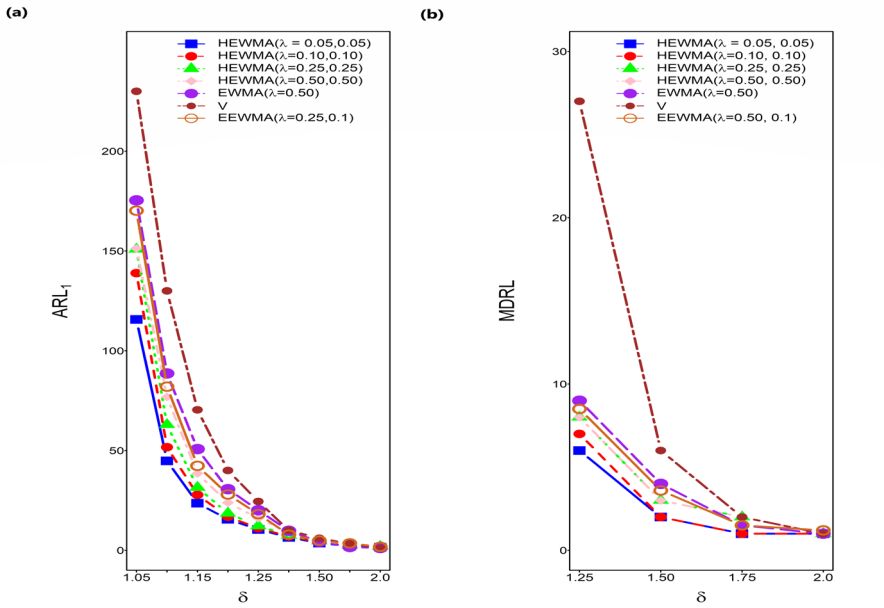


**Fig. 4** **a** ARLs comparison of the proposed $HEWMA_{IM}$ with $EWMA_{IM}$,$V_{IM}$ and $EEWMA_{IM}$ charts on various shift values when n = 6, **b** MDRL comparison on of $HEWMA_{IM}$ with $EWMA_{IM}$,$V_{IM}$ and $EEWMA_{IM}$ charts on varying shifts when n = 9

**Table 7** Overall performance measures of proposed versus existing charts at $ARL_0 = 370$

| | $V_{IM}$ | $EWMA_{IM}$ | $HEWMA_{IM}$ | $V_{IM}$ | $EWMA_{IM}$ | $HEWMA_{IM}$ | $V_{IM}$ | $EWMA_{IM}$ | $HEWMA_{IM}$ |
|---|---|---|---|---|---|---|---|---|---|
| | n = 3 | | | n = 6 | | | n = 9 | | |
| EQL | 71.72 | 61.42 | 52.13 | 58.87 | 58.87 | 55.39 | 54.07 | 54.07 | 52.91 |
| RARL | 1.38 | 1.18 | 1.00 | 1.06 | 1.06 | 1.00 | 1.02 | 1.02 | 1.00 |
| PCI | 3.79 | 2.36 | 1.00 | 1.11 | 1.11 | 1.00 | 1.00 | 1.00 | 1.00 |

Based on this analysis, we accomplish that the proposed $HEWMA_{IM}$ chart outperforms the other competing charts in detecting small and moderate shifts.

## 5 Real Life Applications

The implementation of a control chart on engineering data proves its on-ground performance. The existing applications of control charts in various industries are mentioned to support the study. Prawatya et al. [50] used a control chart to study the Tribocharging process, Chakraborti and Human [16] on nonconforming cans production for orange juice, whereas Senouci et al. [58] on electrostatic separation processes. Further, Hossain and Riaz [23] used on boring machines' lifetime, Wu et al. [70] on GNSS data, and

Taboran et al. [64] applied on manufacturing monitoring of work-piece diameter and deaths during mine explosion time. A hundred applications in diverse industries are available in literature and fields. In this section, we also utilized the two real-life datasets from varied industries and compared the performance of the proposed $\text{HEWMA}_{\text{IM}}$ with $\text{EWMA}_{\text{IM}}$ chart.

### 5.1 Brake Pad Failure Monitoring

To demonstrate the practical implementation of the proposed $\text{HEWMA}_{\text{IM}}$ chart, a lifetime dataset of a car brake pad failure, is used in this study, which is also used by Arafat et al. [8] and Omar et al. [45]. Brake systems in automobiles have been improved over a century and have become incredibly reliable and efficient. It enables the driver to slow down and stop the automobile and keep it on hold when stationary by using the friction force for details, see [46]. Haq et al. [21] described how a poor braking system can lead to accidents, property damage, severe injuries, and even death when it fails by using the past 10 years of accidents from the Wyoming roadway database. Moreover, Jung et al. [28] provided a detailed study on brake field failure. Therefore, significant consideration is given to the design, production, and testing of the braking system components. A brake pad is the essential part of the disc braking system, the standard equipment installed in modern cars, buses, lorries, and heavy vehicles. The distance determines the lifetime of a brake pad traveled since it is established in the vehicle. The data on brake pad longevity was derived from 96 automobiles' left front meter readings. The dataset includes the odometer measurements of every car considered before its original brake pads expired. Each vehicle data measurement is thousands of kilometers. For example, the value 18.9 indicates that the selected car traveled 18,900 km before its first pad expired. The data was split up into 32 samples, each with three observations. Following Anwar et al. [6] and Anwar et al. [7], we introduced a shift of 1.5 in the last thirteen observations in the data set. The goodness of fit was obtained using Kolmogorov–Smirnov (KS) test. The outcome of the test statistic and $p$-value are 0.147 and 0.435. Which suggested that the data set is well-fitted to IM distribution.

The chart parameters of the proposed $\text{HEWMA}_{\text{IM}}$ chart is set on $\lambda_1 = 0.5$, $\lambda_2 = 0.5$, $\text{L} = 3.0945$, and $\boldsymbol{\sigma} = 7.7572$ with $\text{ARL}_0 = 370$. Similarly, the chart parameters of the existing $\text{EWMA}_{\text{IM}}$ control chart are $\lambda_1 = 0.5$, $\text{L} = 3.5558$, and $\boldsymbol{\sigma} = 7.7572$ with $\text{ARL}_0 = 370$, respectively. It is visible that the $\text{HEWMA}_{\text{IM}}$ control chart detects the first OOC signal after the 26th sample, whereas the $\text{EWMA}_{\text{IM}}$ chart detects first OOC signal after the 31st sample, respectively, illustrated in Figs. 5 and 6. In the same manner, the $\text{HEWMA}_{\text{IM}}$ chart detects a total of 7 OOC signals, whereas the existing $\text{EWMA}_{\text{IM}}$ chart detects 1 OOC signal. This indicates the superiority of our proposed $\text{HEWMA}_{\text{IM}}$ charts for detecting early signals as compared to the $\text{EWMA}_{\text{IM}}$ chart.

### 5.2 Carbon Fiber Strength Monitoring

A real-life dataset of carbon fiber strengths is used to determine the $\text{HEWMA}_{\text{IM}}$ chart computing process and performance. A fiber of above 90% carbon content is defined as carbon fiber. The major benefits of carbon fibers compared to other fibers

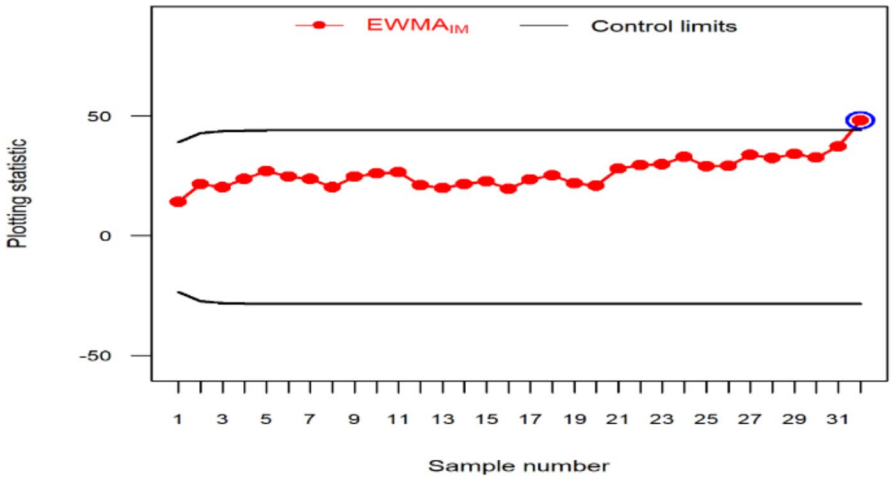


**Fig. 5** Application-1 of the $EWMA_{IM}$ chart at $ARL_0 = 370$

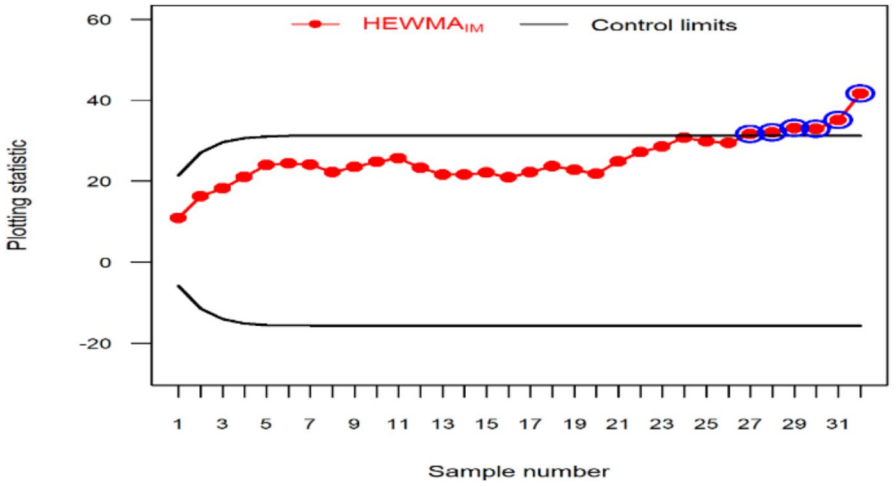


**Fig. 6** Application-1 of the proposed $HEWMA_{IM}$ chart at $ARL_0 = 370$

are having low density, high stiffness, chemical resistance, and tensile strength. The further properties of carbon fiber and manufacturing methods can be found in Chen et al. [17] study. The primary users of carbon fiber include the aviation industry, automotive, wind turbines, defense technologies and civil engineering. The automotive sector is fast growing regarding lightweight structures such as carbon fiber that reduce power consumption. The carbon fiber strength data is taken from Badar and Priest [14], and [60] originally described the application examples. The goodness of fit is measured using the Kolmogorov–Smirnov (KS) test in R software. The probability plot of carbon fiber strength data and the probability value (0.659) of the KS

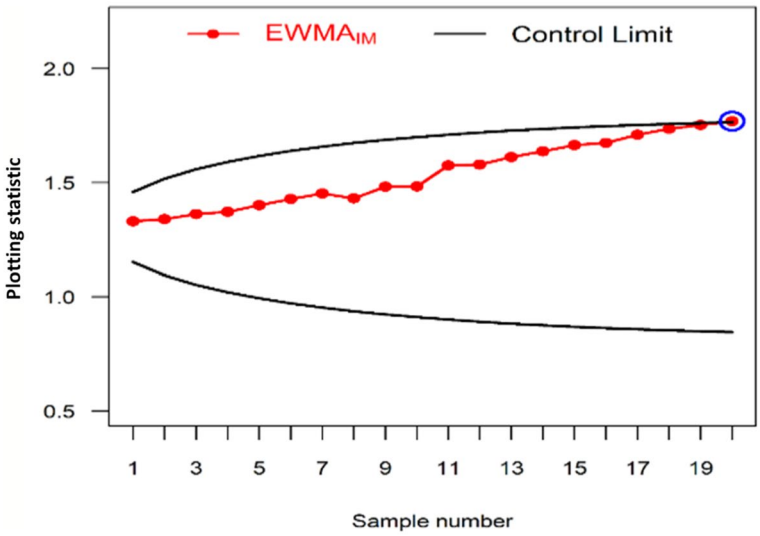


**Fig. 7** Application-2 of the EWMA$_{IM}$ chart at ARL$_0$ = 370

test strongly supported the hypothesis that the dataset follows the IM distribution. The dataset based on 60 strengths is further classified into 20 subgroups, each containing three observations, to use for the proposed HEWMA$_{IM}$ chart. For the OOC scenario, we introduced a small shift ($\delta = 1.1$) in the last ten observations.

The chart parameters of the proposed HEWMA$_{IM}$ chart on carbon fiber strength data is set on $\lambda_1 = 0.05$, $\lambda_2 = 0.05$, L = 1.955, and $\sigma_0 = 1.30548$, ARL$_0$ = 370. Similarly, the chart parameters of the existing EWMA$_{IM}$ control chart are $\lambda_1 = 0.05$, L = 2.523, and $\sigma = 1.30548$ with ARL$_0$ = 370, subsequently. From Figs. 7 and 8, it is clear that the HEWMA$_{IM}$ control chart detects the first OOC signal after the 17th sample, whereas the EWMA$_{IM}$ chart detects the first OOC signal after the 19th sample, respectively. Similarly, the HEWMA$_{IM}$ chart sees 3 OOC signals, whereas the existing EWMA$_{IM}$ chart detects only 1 OOC signal. This also shows the superiority of our proposed HEWMA$_{IM}$ charts for detecting early signals as compared to the EWMA$_{IM}$ chart.

## 6 Conclusion and Recommendations

This study proposed a novel HEWMA$_{IM}$ chart. The proposed chart's run length (RL) characteristics are evaluated using the Monte Carlo simulation approach. The proposed HEWMA$_{IM}$ chart is compared to the charts; the V$_{IM}$, EWMA$_{IM}$ and EEWMA$_{IM}$ charts. The overall performance of the proposed chart is efficient when compared to others by using the extra quadratic loss, performance comparison index, and relative ARL measures. The study's findings unequivocally demonstrate the superiority of the proposed HEWMA$_{IM}$ chart in terms of shift detection capability compared to its competitors. The HEWMA$_{IM}$ chart exhibited

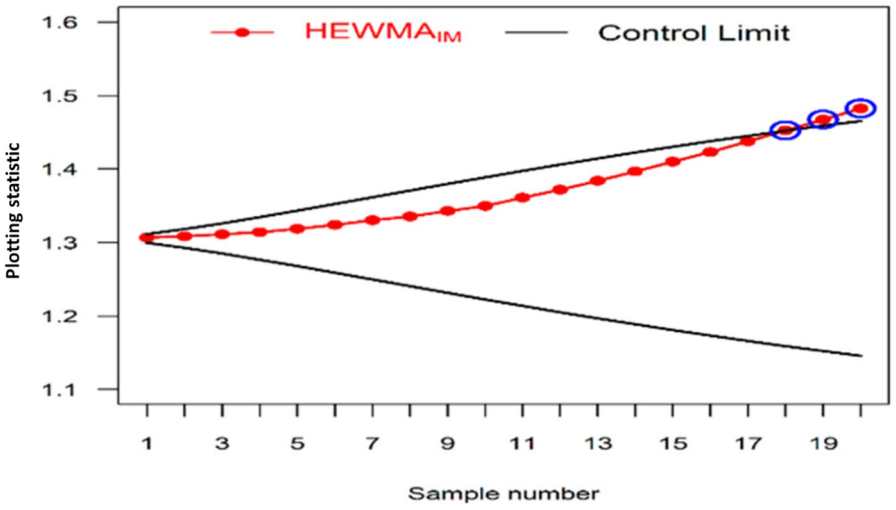


**Fig. 8** Application-2 of the HEWMA$_{IM}$ chart at ARL$_0$ = 370

exceptional performance, particularly in detecting small to moderate shifts, hence, surpassing both competitors. The performance of the chart is examined for both same and different $\lambda$ values for a range of $\lambda_1, \lambda_2$ combinations. When using various $\lambda$ values, the chart responds more quickly to small changes than to big ones. The chart performs better when the $\lambda$ values are the same for detecting moderate shifts. This indicates its efficacy in identifying subtle changes in the monitored process, which is helpful for proactive quality control. Moreover, the practical implementation of the HEWMA$_{IM}$ chart was exemplified through two real-life applications, providing users and practitioners with tangible demonstrations of its effectiveness. These applications provided concrete illustrations of how the HEWMA$_{IM}$ chart can be utilized in various contexts, fostering a deeper understanding of its potential benefits and applicability across different industries. Notably, the performance of the HEWMA$_{IM}$ chart excelled in detecting out-of-control (OOC) signals at an earlier stage compared to existing control charts. This enhanced sensitivity allows for prompt intervention and corrective actions, minimizing the impact of process deviations and improving overall quality control outcomes. The limitation of the study is that it's useful for inverse Maxwell-based processes and related skewed processes.

Overall, the study's findings endorse the effectiveness and practicality of the proposed HEWMA$_{IM}$ chart, positioning it as a robust tool for efficient and proactive process monitoring and control, surpassing its competitors in shift detection, real-life application viability, and early OOC signal detection. The proposed chart presents a compelling solution for manufacturers, offering many benefits that result in time and cost savings and improved operational efficiency. Its versatile applicability spans numerous industries, making it relevant and impactful at various levels. The chart can enhance decision-making and resource allocation in government sectors, such as military and public services. Its implementation in production, including

automotive, electronics, beverages, and food manufacturing, can lead to streamlined processes, higher product quality, and increased customer satisfaction.

Furthermore, the chart's value extends beyond these sectors. In construction, for instance, it can aid in project management, ensuring timely completion and adherence to quality standards. In healthcare, it can be instrumental in monitoring critical parameters, optimizing patient care, and improving patient safety [13, 66–69]. In energy, retail, and services, the chart's application holds the potential to drive efficiency gains, cost reductions, and enhanced performance metrics. Moreover, this research opens avenues for further exploration. It lays the foundation for extending the principles of memory control charts to monitor non-normal processes, providing a broader scope for performance evaluation and anomaly detection. By delving deeper into this aspect, researchers can contribute to advancing quality control practices across diverse industries, ultimately leading to improved productivity, profitability, and customer satisfaction.

**Acknowledgements** The author thanks the Department of Health Managment & Institute of Medical Artificial Intelligence, The Second Affiliated Hospital, (School of Mathematics and Statistics) Xi'an Jiaotong University, Xi'an, China, and the Department of Statistics, University of WAH, Pakistan for offering research facilities.

**Author Contribution** MW contributed to the idea design, data collection, simulation findings and implementation of the overall research. ZR and SMA supported in the analysis and writing of the manuscript. GM and ZR supported in the revision. SHX supervised this research.

**Funding** No funding was received to conduct this study.

**Data Availability** The datasets supporting the study's findings are available on request from the corresponding author. Moreover, the datasets used have already been verified in previous publications, which are referenced in the above relevant section.

## Declarations

**Conflict of Interest** All authors report no conflict of interest relevant to this article.



## References

1. Abbasi, S.A.: Efficient control charts for monitoring process CV using auxiliary information. IEEE Access **8**, 46176–46192 (2020). https://doi.org/10.1109/ACCESS.2020.2977833
2. Ahsan, M., Mashuri, M., Khusna, H.: Comparing the performance of Kernel PCA mix chart with PCA mix chart for monitoring mixed quality characteristics. Sci. Rep. **12**(1), 15723 (2022). https://doi.org/10.1038/s41598-022-20122-w

3. Alevizakos, V., Chatterjee, K., Koukouvinos, C.: Nonparametric triple exponentially weighted moving average signed-rank control chart for monitoring shifts in the process location. Qual. Reliabil. Eng. Int. **37**(6), 2622–2645 (2021). https://doi.org/10.1002/qre.2879
4. Ali, R., Haq, A.: New memory-type dispersion control charts. Qual. Reliabil. Eng. Int. **33**(8), 2131–2149 (2017). https://doi.org/10.1002/qre.2174
5. Alnssyan, B., Ahmad, Z., Malela-Majika, J.-C., Seong, J.-T., Shafik, W.: On the identifiability and statistical features of a new distributional approach with reliability applications. AIP Adv. **13**(12), 125211 (2023). https://doi.org/10.1063/5.0178555
6. Anwar, S.M., Aslam, M., Zaman, B., Riaz, M.: An enhanced double homogeneously weighted moving average control chart to monitor process location with application in automobile field. Qual. Reliabil. Eng. Int. **38**, 174 (2021). https://doi.org/10.1002/qre.2966
7. Anwar, S.M., Aslam, M., Zaman, B., Riaz, M.: Mixed memory control chart based on auxiliary information for simultaneously monitoring of process parameters: an application in glass field. Comput. Ind. Eng. **156**, 107284 (2021). https://doi.org/10.1016/j.cie.2021.107284
8. Arafat, S.Y., Hossain, M.P., Ajadi, J.O., Riaz, M.: On the development of EWMA control chart for inverse Maxwell distribution. J. Test. Eval. **49**(2), 1086–1103 (2019). https://doi.org/10.1520/JTE20190082
9. Arslan, M., Anwar, S.M., Lone, S.A., Rasheed, Z., Khan, M., Abbasi, S.A.: Improved adaptive EWMA control chart for process location with applications in groundwater physicochemical parameters and glass manufacturing industry. PLoS ONE **17**(8), e0272584 (2022). https://doi.org/10.1371/journal.pone.0272584
10. Ashraf, A., Ali, S., Shah, I.: Online disease risk monitoring using DEWMA control chart. Expert Syst. Appl. **180**, 115059 (2021). https://doi.org/10.1016/j.eswa.2021.115059
11. Aslam, M., Anwar, S.M., Khan, M., Abiodun, N.L., Rasheed, Z.: Efficient auxiliary information-based control charting schemes for the process dispersion with application of glass manufacturing industry. Math. Probl. Eng. **2022**, 1265204 (2022). https://doi.org/10.1155/2022/1265204
12. Aslam, M., Khan, N., Jun, C.H.: A hybrid exponentially weighted moving average chart for COM-Poisson distribution. Trans. Inst. Meas. Control. **40**(2), 456–461 (2016). https://doi.org/10.1177/0142331216659920
13. Aslam, M.U., Xu, S., Noor-ul-Amin, M., Hussain, S., Waqas, M.: Fuzzy control charts for individual observations to analyze variability in health monitoring processes. Appl. Soft Comput. **164**, 111961 (2024). https://doi.org/10.1016/j.asoc.2024.111961
14. Badar, M.G., Priest, A.M.: Statistical aspects of fibre and bundle strength in hybrid composites. In Hayashi, T., Kawata, K., Umekawa S. (eds) Progress in Science and Engineering Composites, pp. 1129–1136 (1982)
15. Boaventura, L.L., Ferreira, P.H., Fiaccone, R.L.: On flexible statistical process control with artificial intelligence: classification control charts. Expert Syst. Appl. **194**, 116492 (2022). https://doi.org/10.1016/j.eswa.2021.116492
16. Chakraborti, S., Human, S.W.: Parameter estimation and performance of the $p$-chart for attributes data. IEEE Trans. Reliab. **55**(3), 559–566 (2006). https://doi.org/10.1109/TR.2006.879662
17. Chen, A.Y., Baehr, S., Turner, A., Zhang, Z., Gu, G.X.: Carbon-fiber reinforced polymer composites: a comparison of manufacturing methods on mechanical properties. Int. J. Lightw. Mater. Manuf. **4**(4), 468–479 (2021). https://doi.org/10.1016/j.ijlmm.2021.04.001
18. De la Torre-Gutiérrez, H., Pham, D.: A control chart pattern recognition system for feedback-control processes. Expert Syst. Appl. **138**, 112826 (2019). https://doi.org/10.1016/j.eswa.2019.112826
19. Haq, A.: A new hybrid exponentially weighted moving average control chart for monitoring process mean. Qual. Reliabil. Eng. Int. **29**(7), 1015–1025 (2013). https://doi.org/10.1002/qre.1453
20. Haq, A.: A new hybrid exponentially weighted moving average control chart for monitoring process mean: discussion. Qual. Reliabil. Eng. Int. **33**(7), 1629–1631 (2017). https://doi.org/10.1002/qre.2092
21. Haq, M.T., Ampadu, V.-M.K., Ksaibati, K.: An investigation of brake failure related crashes and injury severity on mountainous roadways in Wyoming. J. Saf. Res. (2022). https://doi.org/10.1016/j.jsr.2022.10.003
22. Hossain, M.P., Omar, M.H., Riaz, M.: New V control chart for the Maxwell distribution. J. Stat. Comput. Simul. **87**(3), 594–606 (2017). https://doi.org/10.1080/00949655.2016.1222391
23. Hossain, M.P., Riaz, M.: On designing a new VEWMA control chart for efficient process monitoring. Comput. Ind. Eng. **162**, 107751 (2021). https://doi.org/10.1016/j.cie.2021.107751

24. Hossain, M.P., Sanusi, R.A., Omar, M.H., Riaz, M.: On designing Maxwell CUSUM control chart: an efficient way to monitor failure rates in boring processes. Int. J. Adv. Manuf. Technol. **100**(5), 1923–1930 (2019). https://doi.org/10.1007/s00170-018-2679-1
25. Hussain, S., Mei, S., Riaz, M., Abbasi, S.A.: On phase-I monitoring of process location parameter with auxiliary information-based median control charts. Mathematics **8**(5), 706 (2020)
26. Jain, A., Sarvepalli, P., Bhashyam, S., Kannu, A.P.: Algorithms for change detection with sparse signals. IEEE Trans. Signal Process. **68**, 1331–1345 (2020). https://doi.org/10.1109/TSP.2020.2973115
27. Jalilibal, Z., Karavigh, M.H.A., Maleki, M.R., Amiri, A.: Control charting methods for monitoring high dimensional data streams: a conceptual classification scheme. Comput. Ind. Eng. **191**, 110141 (2024). https://doi.org/10.1016/j.cie.2024.110141
28. Jung, W., Kim, G., & Ismail, A.: Reliability improvement of brake pads. In: Case study. 2012 International Conference on Quality, Reliability, Risk, Maintenance, and Safety Engineering (2012, 15–18 June 2012)
29. Khan, I., Khan, D.M., Noor-ul-Amin, M., Khalil, U., Alshanbari, H.M., Ahmad, Z.: Hybrid EWMA control chart under bayesian approach using ranked set sampling schemes with applications to hard-bake process. Appl. Sci. **13**(5), 2837 (2023)
30. Khan, M., Aslam, M., Anwar, S.M., Zaman, B.: A robust hybrid exponentially weighted moving average chart for monitoring time between events. Qual. Reliabil. Eng. Int. **38**(2), 895–923 (2022). https://doi.org/10.1002/qre.3021
31. Khan, M., Rasheed, Z., Anwar, S., Namangale, J.: Triple homogeneously weighted moving average charts for monitoring process dispersion. Math. Probl. Eng. **2023**, 1–34 (2023). https://doi.org/10.1155/2023/6996280
32. Khoo, M.B.C., Wong, V.H.: A double moving average control chart. Commun. Stat. Simul. Comput. **37**, 1696–1708 (2008)
33. Khoo, M.B.C., Wu, Z., Chen, C.-H., Yeong, K.W.: Using one EWMA chart to jointly monitor the process mean and variance. Comput. Stat. **25**(2), 299–316 (2010). https://doi.org/10.1007/s00180-009-0177-5
34. Kusum, L.S., Srivastava, R.S.: Inverse Maxwell distribution as a survival model, genesis and parameter estimation. Res. J. Math. Stat. Sci. **2**(7), 23–28 (2014)
35. Liu, X., Khan, M., Rasheed, Z., Anwar, S.M., Arslan, M.: New hybrid EWMA charts for efficient process dispersion monitoring with application in automobile industry. Comput. Model. Eng. Sci. **131**, 1–25 (2022)
36. Liu, X., Khan, M., Rasheed, Z., Anwar, S.M., Arslan, M.: New hybrid EWMA charts for efficient process dispersion monitoring with application in automobile industry. CMES Comput. Model. Eng. Sci. **131**(2), 1171–1195 (2022)
37. Liu, Z., Wang, S., Gu, X., Li, Z., Dong, Q., Cui, B.: Application of a novel EWMA-ϕ chart on quality control in asphalt mixtures production. Constr. Build. Mater. **323**, 126264 (2022). https://doi.org/10.1016/j.conbuildmat.2021.1262644
38. Mahmoud, M.A., Woodall, W.H.: An evaluation of the double exponentially weighted moving average control chart. Commun. Stat. Simul. Comput. **39**(5), 933–949 (2010). https://doi.org/10.1080/03610911003663907
39. Malela-Majika, J.-C., Shongwe, S.C., Aslam, M., Abbasi, S.A.: Robust distribution-free hybrid exponentially weighted moving average schemes based on simple random sampling and ranked set sampling techniques. Math. Probl. Eng. **2021**, 4035011 (2021). https://doi.org/10.1155/2021/4035011
40. Maqsood, M., Sanaullah, A., Mahmood, Y., Al-Rezami, A.Y., Abdalla, M.Z.M.: Efficient control chart-based monitoring of scale parameter for a process with heavy-tailed non-normal distribution. AIMS Math. **8**(12), 30075–30101 (2023). https://doi.org/10.3934/math.20231538
41. Munir, T., Hu, X., Kauppila, O., Bergquist, B.: Effect of measurement uncertainty on combined quality control charts. Comput. Ind. Eng. **175**, 108900 (2023). https://doi.org/10.1016/j.cie.2022.108900
42. Ng, P.S., Goh, S.Y., Saha, S., & Yeong, W.C.: An enhanced double EWMA chart for monitoring the process mean shifts. In: Proceedings of the 12th International Conference on Robotics, Vision, Signal Processing and Power Applications, Singapore (2024)
43. Noor-ul-Amin, M., Aslam, I., Feroze, N.: Joint monitoring of mean and variance using Max-EWMA for Weibull process. Commun. Stat. Simul. Comput. **52**(7), 3257–3272 (2023). https://doi.org/10.1080/03610918.2021.1931322

44. Noor, S., Noor-ul-Amin, M., Mohsin, M., Ahmed, A.: Hybrid exponentially weighted moving average control chart using Bayesian approach. Commun. Stat. Theory Methods (2020). https://doi.org/10.1080/03610926.2020.1805765
45. Omar, M.H., Arafat, S.Y., Hossain, M.P., Riaz, M.: Inverse Maxwell distribution and statistical process control: an efficient approach for monitoring positively skewed process. Symmetry **13**(2), 189 (2021)
46. Orłowicz, A.W., Mróz, M., Wnuk, G., Markowska, O., Homik, W., Kolbusz, B.J.A.O.F.E.: Coefficient of friction of a brake disc-brake pad friction couple. Arch Found Eng **16**, 196–200 (2016)
47. Page, E.S.: Continuous inspection schemes. Biometrika **41**, 100–115 (1954)
48. Pear Hossain, M., Hafidz Omar, M., Riaz, M.: Estimation of mixture Maxwell parameters and its possible industrial application. Comput. Ind. Eng. **107**, 264–275 (2017). https://doi.org/10.1016/j.cie.2017.03.023
49. Phanthuna, P., Areepong, Y., Sukparungsee, S.: Exact run length evaluation on a two-sided modified exponentially weighted moving average chart for monitoring process mean. Comput. Model. Eng. Sci. **127**(1), 23 (2021). https://doi.org/10.32604/cmes.2021.013810
50. Prawatya, Y.E., Senouci, K., Zeghloul, T., Neagoe, M.B., Dascalescu, L., Medles, K.: Control charts for statistical process control of the tribocharging of polymer slabs in frictional sliding contact. IEEE Trans. Ind. Appl. **55**(5), 5253–5260 (2019). https://doi.org/10.1109/TIA.2019.2923165
51. Rasheed, Z., Khan, M., Abiodun, N.L., Anwar, S.M., Khalaf, G., Abbasi, S.A.: Improved nonparametric control chart based on ranked set sampling with application of chemical data modelling. Math. Probl. Eng. **2022**, 7350204 (2022). https://doi.org/10.1155/2022/7350204
52. Rasheed, Z., Khan, M., Anwar, S., Aslam, M.U., Lone, S., Almutlak, S.: Designing an efficient adaptive EWMA model for normal process with engineering applications. Ain Shams Eng. J. (2024). https://doi.org/10.1016/j.asej.2024.102904
53. Rasheed, Z., Zhang, H., Anwar, S.M., Zaman, B.: Homogeneously mixed memory charts with application in the substrate production process. Math. Probl. Eng. **2021**, 2582210 (2021). https://doi.org/10.1155/2021/2582210
54. Riaz, M., Ajadi, J., Hossain, M.P., Arafat, S.Y.: On the development of EWMA control chart for inverse Maxwell distribution. J. Test. Eval. (2019). https://doi.org/10.1520/JTE20190082
55. Roberts, S.W.: Control chart tests based on geometric moving averages. Technometrics **1**(3), 239–250 (1959)
56. Saghir, A., Aslam, M., Faraz, A., Ahmad, L., Heuchenne, C.: Monitoring process variation using modified EWMA. Qual Rehabil Eng **36**(1), 328–339 (2020). https://doi.org/10.1002/qre.2576
57. Sarwar, M.A., Noor-ul-Amin, M., Khan, I., Ismail, E.A.A., Sumelka, W., Nabi, M.: A Weibull process monitoring with AEWMA control chart: an application to breaking strength of the fibrous composite. Sci. Rep. **13**(1), 19873 (2023). https://doi.org/10.1038/s41598-023-47159-9
58. Senouci, K., Bendaoud, A., Tilmatine, A., Medles, K., Das, S., Dascalescu, L.: Multivariate statistical process control of electrostatic separation processes. IEEE Trans. Ind. Appl. **45**(3), 1079–1085 (2009). https://doi.org/10.1109/TIA.2009.2018939
59. Shafqat, A., Aslam, M., Saleem, M., Abbas, Z.: The new neutrosophic double and triple exponentially weighted moving average control charts. Comput. Model. Eng. Sci. **129**(1), 373 (2021). https://doi.org/10.32604/cmes.2021.016772
60. Shah, F., Khan, Z., Aslam, M., Kadry, S.: Statistical development of the VSQ-control chart for extreme data with an application to the carbon fiber industry. Math. Eng. (2021). https://doi.org/10.1155/2021/9766986
61. Shamma, S.E., Shamma, A.K.: Development and evaluation of control charts using double exponentially weighted moving averages. Int. J. Qual. Reliabil. Manag. **9**(6), 18–25 (1992)
62. Shewhart, W.A.: Economic control of quality manufactured product (1931)
63. Singh, K.L., Srivatsava, R.S.: Estimation of the parameter in the size-biased inverse maxwell distribution. Int. J. Stat. Math. **10**, 52–55 (2014)
64. Taboran, R., Sukparungsee, S., Areepong, Y.: A new nonparametric Tukey MA-EWMA control charts for detecting mean shifts. IEEE Access **8**, 207249–207259 (2020). https://doi.org/10.1109/ACCESS.2020.3037293
65. Tomer, S.K., Panwar, M.S.: A review on inverse Maxwell distribution with its statistical properties and applications. J. Stat. Theory Pract. **14**(3), 33 (2020). https://doi.org/10.1007/s42519-020-00100-z

66. Waqas, M., Xu, S.H., Anwar, S.M., Rasheed, Z., Shabbir, J.: The optimal control chart selection for monitoring COVID-19 phases: a case study of daily deaths in the USA. Int. J. Qual. Health Care **35**(3), mzad058 (2023). https://doi.org/10.1093/intqhc/mzad058
67. Waqas, M., Xu, S.H., Hussain, S., Aslam, M.U.: Control charts in healthcare quality monitoring: a systematic review and bibliometric analysis. Int. J. Qual. Health Care **36**(3), mzae060 (2024). https://doi.org/10.1093/intqhc/mzae060
68. Waqas, M., Xu, S.H., Aslam, M.U., Hussain, S., Masengo, G.: Transforming healthcare performance monitoring – A cutting-edge approach with generalized additive profiles: GAMs for healthcare quality monitoring. Medicine **103**(37), e39328 (2024). https://doi.org/10.1097/MD.0000000000039328
69. Waqas, M., Xu, S.H., Aslam, M.U., Hussain, S., Shahzad, K., Masengo, G.: Global contribution of statistical control charts to epidemiology monitoring: A 23-year analysis with optimized EWMA real-life application on COVID-19. Medicine **103**(27) e38766 (2024). https://doi.org/10.1097/MD.0000000000038766
70. Wu, H., Dai, Y., Wang, C., Xu, X.-W., Jiang, X.-M.: Identification and forewarning of GNSS deformation information based on a modified EWMA control chart. Measurement **160**, 107854 (2020). https://doi.org/10.1016/j.measurement.2020.107854
71. Yadpirun Supharakonsakun, Y.A., Sukparungsee, S.: Monitoring the process mean of a modified ewma chart for arma(1,1) process and its application. Suranaree J. Sci. Technol. **27**(4), 1–11 (2020)
72. Yang, S.F., Shen, L.: Loss-based control charts for monitoring non-normal process data. IEEE Access **8**, 91163–91169 (2020). https://doi.org/10.1109/ACCESS.2020.2989400
73. Zaka, A., Akhter, A.S., Jabeen, R., Sanaullah, A.: Control charts for the shape parameter of power function distribution under different classical estimators. Comput. Model. Eng. Sci. **127**(3), 1201 (2021). https://doi.org/10.32604/cmes.2021.014477
74. Zwetsloot, I.M., Mahmood, T., Woodall, W.H.: Multivariate time-between-events monitoring: an overview and some overlooked underlying complexities. Qual. Eng. **33**(1), 13–25 (2021). https://doi.org/10.1080/08982112.2020.1788717

## Authors and Affiliations

**Muhammad Waqas[1,7] · Song Hua Xu[2,3] · Syed Masroor Anwar[4] · Zahid Rasheed[5] · Gilbert Masengo[6]**

✉ Gilbert Masengo
dr.data2013@gmail.com
https://www.researchgate.net/profile/Gilbert-Masengo

Muhammad Waqas
wakas.brw@gmail.com
https://www.researchgate.net/profile/Muhammad-Waqas-Ch

Song Hua Xu
songhuaxu@126.com

Syed Masroor Anwar
masroorstatistics@gmail.com
https://www.researchgate.net/profile/Syed-Anwar-7

Zahid Rasheed
zahidrasheed99@gmail.com
https://www.researchgate.net/profile/Zahid-Rasheed-2

1 School of Mathematics and Statistics, Xi'an Jiaotong University, Xi'an 710049, China

2 Department of Computer Science, Yale University, New Haven, USA

3 Institute of Medical Artificial Intelligence, The Second Affiliated Hospital, Xi'an Jiaotong University, Xi'an 710049, China

[4] Department of Statistics, University of Azad Jammu and Kashmir, Muzaffarabad 13100, Pakistan

[5] Department of Mathematics, Women University of Azad Jammu and Kashmir Bagh, Bagh, Pakistan

[6] Department of Mechanical Engineering, Rwanda Polytechnic/Integrated Polytechnic Regional College (IPRC) Karongi, Kigali, Rwanda

[7] Department of Statistics, University of WAH, Wah, Pakistan